HANOI UNIVERSITY OF SCIENCE AND TECHNOLOGY
SCHOOL OF ELECTRONICS AND TELECOMMUNICATIONS

GRADUATION THESIS

Topic:

OFDM COMMUNICATION: ICI compensation in HSR OFDM, compressed sensing channel estimation and chaotic subcarriers

Student: VU NHAT MINH

Telecommunication-AP-K56

Advisor: Assoc. Prof. VU VAN YEM

Critical officer:

Hanoi, June 2016

HANOI UNIVERSITY OF SCIENCE AND TECHNOLOGY
SCHOOL OF ELECTRONICS AND TELECOMMUNICATIONS

GRADUATION THESIS

Topic:

OFDM COMMUNICATION: ICI compensation in HSR OFDM, compressed sensing channel estimation and chaotic subcarriers

Student: VU NHAT MINH

Telecommunication-AP-K56

Advisor: Assoc. Prof. VU VAN YEM

Critical officer:

Hanoi, June 2016

Đánh giá quyển đồ án tốt nghiệp
(Dùng cho giảng viên hướng dẫn)

Giảng viên đánh giá: **Assoc. Prof. Vũ Văn Yêm**
Họ và tên sinh viên: **Vũ Nhật Minh** MSSV: 20111873
Tên đồ án: **OFDM communication: ICI compensation in HSR OFDM, compressed sensing channel estimation and chaotic subcarriers**

Chọn các mức điểm phù hợp cho sinh viên trình bày theo các tiêu chí dưới đây:
Rất kém (1); Kém (2); Đạt (3); Giỏi (4); Xuất sắc (5)

Có sự kết hợp giữa lý thuyết và thực hành (20)						
1	Nêu rõ tính cấp thiết và quan trọng của đề tài, các vấn đề và các giả thuyết (bao gồm mục đích và tính phù hợp) cũng như phạm vi ứng dụng của đồ án	1	2	3	4	5
2	Cập nhật kết quả nghiên cứu gần đây nhất (trong nước/quốc tế)	1	2	3	4	5
3	Nêu rõ và chi tiết phương pháp nghiên cứu/giải quyết vấn đề	1	2	3	4	5
4	Có kết quả mô phỏng/thực nghiệm và trình bày rõ ràng kết quả đạt được	1	2	3	4	5
Có khả năng phân tích và đánh giá kết quả (15)						
5	Kế hoạch làm việc rõ ràng bao gồm mục tiêu và phương pháp thực hiện dựa trên kết quả nghiên cứu lý thuyết một cách có hệ thống	1	2	3	4	5
6	Kết quả được trình bày một cách logic và dễ hiểu, tất cả kết quả đều được phân tích và đánh giá thỏa đáng.	1	2	3	4	5
7	Trong phần kết luận, tác giả chỉ rõ sự khác biệt (nếu có) giữa kết quả đạt được và mục tiêu ban đầu đề ra đồng thời cung cấp lập luận để đề xuất hướng giải quyết có thể thực hiện trong tương lai.	1	2	3	4	5
Kỹ năng viết (10)						
8	Đồ án trình bày đúng mẫu quy định với cấu trúc các chương logic và đẹp mắt (bảng biểu, hình ảnh rõ ràng, có tiêu đề, được đánh số thứ tự và được giải thích hay đề cập đến trong đồ án, có căn lề, dấu cách sau dấu chấm, dấu phẩy v.v), có mở đầu chương và kết luận chương, có liệt kê tài liệu tham khảo và có trích dẫn đúng quy định	1	2	3	4	5
9	Kỹ năng viết xuất sắc (cấu trúc câu chuẩn, văn phong khoa học, lập luận logic và có cơ sở, từ vựng sử dụng phù hợp v.v.)	1	2	3	4	5
Thành tựu nghiên cứu khoa học (5) (chọn 1 trong 3 trường hợp)						
10a	Có bài báo khoa học được đăng hoặc chấp nhận đăng/đạt giải SVNC khoa học giải 3 cấp Viện trở lên/các giải thưởng khoa học (quốc tế/trong nước) từ giải 3 trở lên/ Có đăng ký bằng phát minh sáng chế	5				
10b	Được báo cáo tại hội đồng cấp Viện trong hội nghị sinh viên nghiên cứu khoa học nhưng không đạt giải từ giải 3 trở lên/Đạt giải khuyến khích trong các kỳ thi quốc gia và quốc tế khác về chuyên ngành như TI contest.	2				
10c	Không có thành tích về nghiên cứu khoa học	0				
Điểm tổng		**/50**				
Điểm tổng quy đổi về thang 10						

3. Nhận xét thêm của Thầy/Cô (*giảng viên hướng dẫn nhận xét về thái độ và tinh thần làm việc của sinh viên****)***

.....
.....
.....
.....
.....

Ngày / / 201

Người nhận xét

(Ký và ghi rõ họ tên)

Đánh giá quyển đồ án tốt nghiệp
(Dùng cho cán bộ phản biện)

Giảng viên đánh giá: ……
Họ và tên sinh viên: **Vũ Nhật Minh** MSSV: 20111873
Tên đồ án: **OFDM communication: ICI compensation in HSR OFDM, compressed sensing channel estimation and chaotic subcarriers**

Chọn các mức điểm phù hợp cho sinh viên trình bày theo các tiêu chí dưới đây:
Rất kém (1); Kém (2); Đạt (3); Giỏi (4); Xuất sắc (5)

Có sự kết hợp giữa lý thuyết và thực hành (20)						
1	Nêu rõ tính cấp thiết và quan trọng của đề tài, các vấn đề và các giả thuyết (bao gồm mục đích và tính phù hợp) cũng như phạm vi ứng dụng của đồ án	1	2	3	4	5
2	Cập nhật kết quả nghiên cứu gần đây nhất (trong nước/quốc tế)	1	2	3	4	5
3	Nêu rõ và chi tiết phương pháp nghiên cứu/giải quyết vấn đề	1	2	3	4	5
4	Có kết quả mô phỏng/thực nghiệm và trình bày rõ ràng kết quả đạt được	1	2	3	4	5
Có khả năng phân tích và đánh giá kết quả (15)						
5	Kế hoạch làm việc rõ ràng bao gồm mục tiêu và phương pháp thực hiện dựa trên kết quả nghiên cứu lý thuyết một cách có hệ thống	1	2	3	4	5
6	Kết quả được trình bày một cách logic và dễ hiểu, tất cả kết quả đều được phân tích và đánh giá thỏa đáng.	1	2	3	4	5
7	Trong phần kết luận, tác giả chỉ rõ sự khác biệt (nếu có) giữa kết quả đạt được và mục tiêu ban đầu đề ra đồng thời cung cấp lập luận để đề xuất hướng giải quyết có thể thực hiện trong tương lai.	1	2	3	4	5
Kỹ năng viết (10)						
8	Đồ án trình bày đúng mẫu quy định với cấu trúc các chương logic và đẹp mắt (bảng biểu, hình ảnh rõ ràng, có tiêu đề, được đánh số thứ tự và được giải thích hay đề cập đến trong đồ án, có căn lề, dấu cách sau dấu chấm, dấu phẩy v.v), có mở đầu chương và kết luận chương, có liệt kê tài liệu tham khảo và có trích dẫn đúng quy định	1	2	3	4	5
9	Kỹ năng viết xuất sắc (cấu trúc câu chuẩn, văn phong khoa học, lập luận logic và có cơ sở, từ vựng sử dụng phù hợp v.v.)	1	2	3	4	5
Thành tựu nghiên cứu khoa học (5) (chọn 1 trong 3 trường hợp)						
10a	Có bài báo khoa học được đăng hoặc chấp nhận đăng/đạt giải SVNC khoa học giải 3 cấp Viện trở lên/các giải thưởng khoa học (quốc tế/trong nước) từ giải 3 trở lên/ Có đăng ký bằng phát minh sáng chế	5				
10b	Được báo cáo tại hội đồng cấp Viện trong hội nghị sinh viên nghiên cứu khoa học nhưng không đạt giải từ giải 3 trở lên/Đạt giải khuyến khích trong các kỳ thi quốc gia và quốc tế khác về chuyên ngành như TI contest.	2				
10c	Không có thành tích về nghiên cứu khoa học	0				
Điểm tổng		**/50**				
Điểm tổng quy đổi về thang 10						

3. Nhận xét thêm của Thầy/Cô

.....
.....
.....
.....
.....

Ngày / / 201

Người nhận xét

(Ký và ghi rõ họ tên)

FOREWORD

In recent years, Orthogonal frequency division multiplexing (OFDM) has been developed as a popular scheme for wideband digital communication to apply in numerous applications. Apparently, OFDM is robust against Inter-Symbol-Interference (ISI) because of the long symbol duration. However, for mobile application, the variations of communication channel introduce Inter-carrier-Interference (ICI), which lowers the overall performance.

The breakdown due to ICI is more severe when antennas speed, OFDM symbol duration or carrier frequency increases. Especially, in High-speed Railway (HSR) system, the train speed can reach up to 300-400 kilometers per hour. As a result, more technical requirements are put forward for mobile communication system. Two common problems caused by high mobility are over-frequent handover and high Doppler frequency shift. Distributed antenna system (DAS) which has been introduced in [1,2] is one practical solution to the handover problem. In DAS, several linearly arranged remote radio units (RRU) connecting with one control center communicate with a high speed mobile station (MS). This configuration introduces two independent Doppler shifts from two RRUs, which require further investigations.

In this research, we propose a method to estimate the frequency shift based on a preamble frame of data in communication link between RRUs and MS. This method is an improvement of MUSIC algorithm in [3].

In addition, we realize that the problem can be generalized into a channel estimation problem in OFDM communications with ICI. Thus, we investigated the usage of compressed sensing and manifold approximation into HSR-OFDM.

Lastly, we implement chaotic subcarrier modulation on OFDM symbol to enhance the privacy and security of communication link. In this thesis, we focus on evaluating the performance of chaotic subcarrier under different conditions and modulation schemes. The results point out that the proposed system not only solves the security concern but also maintains the same performance as the bit-error-rate is the same as conventional system.

In the process of preparing, I received kindly support from my advisor Assoc. Prof. Vu Van Yem and all the members in the lab. I would like to thank Assoc. Prof. Vu Van Yem for his help to complete this thesis.

ASTRACT

OFDM is substantial against Inter-symbol-interference due to long symbol duration. However. Inter-carrier interference caused by high Doppler frequency shift has severe impact on OFDM in case of high channel variations. In this project we investigate the Inter-symbol-interference mitigation scheme by utilizing the estimation and pre-compensation of high Doppler shifts in High-speed Railway systems with distributed remote radio units. In addition, we implement another algorithm to estimate the channels in High-speed Railway based on compressed sensing theory. Lastly, a scheme of interleaving chaotic subcarriers on OFDM symbol before transmission are also examined in this thesis.

REPORT SUMMARY

In this thesis, we investigated different aspects of OFDM communication. Our work is divided into three main parts which are deeply examined in CHAPTER 2, 3 and 4. CHAPER 1 is the overview background knowledge for this thesis. It not only provides readers the structure of this report, but also specifies the current states of each area or research related to this thesis. CHAPTER 2 is about the Carrier Frequency Offset (CFO) estimation. The compressed sensing based channel estimation method is explained in CHAPTER 3. Lastly, a proposed method of interleaving chaotic subcarriers modulation on OFDM symbol is illustrated in CHAPTER 4. The last three chapter all contain the brief mathematical backgrounds, system models and simulations of corresponding proposed methods.

TABLE CONTENT

LIST OF FIGURES

LIST OF TABLES

LIST OF ABBREVIATIONS

4G	Fourth generation
ADC	Analog-to-digital
AOA	Angle of arrival
AOA	Angle of arrival
AWGN	Additive white Gaussian noise
BER	Bit error rate
BPSK	Binary phase-shift keying
BPSK	Binary phase-shift keying
BS	Base station
CFO	Carrier frequency offset
CIR	Channel impulse response
CP	Cyclic-prefix
CS	Compressed sensing
DAC	Digital-to-analog
DBM	Discrete Baker mapping
DFT	Discrete Fourier transform
DSL	Digital subscriber line
Eb/N0	Energy per bit to noise power spectral density ratio
FEC	Forward error correction
HSR	High-speed railway

HSR	High speed railway
ICI	Inter-carrier-interference
IDFT	Inverse Discrete Fourier transform
ISI	Inter-symbol-interference
LOS	Line of Sight
LTE-R	Long Term Evolution for Railway
MIMO	Multiple input, multiple output
ML	Maximum likelihood
ms	Mobile station
MUSIC	Multiple signal classification
OFDM	Orthogonal frequency division multiplexing
OFDMA	Orthogonal frequency division multiple access
P/S	Parallel to Serial
PSD	Power spectral density
QAM	Quadrature amplitude modulation
QPSK	Quadrature phase shift keying
RRU	Remote radio units
S/P	Serial to Parallel
SISO	Single-input single-output
SM	Spatially multiplexed
SNR	Signal-to-noise ratio
SSC	Subspace clustering
WSS	Wide-sense Stationary
ZP	Zero-padding

CHAPTER 1

OVERVIEW

1.1 OFDM transmission

Orthogonal frequency division multiplexing (OFDM) is a method of encoding digital data on multiple sub-carriers. OFDM has been developed as a prevalent scheme for wideband digital communication, installed in applications such as digital television and audio broadcasting, DSL Internet access, wireless networks, powerline networks, and 4G mobile communications.

In OFDM, a large number of closely spaced orthogonal sub-carriers is modulated with conventional modulation techniques (such as BPSK or QPSK) at low symbol rate. The total data rate is analogous to conventional single-carrier modulation schemes in the same bandwidth.

The major advantage of OFDM is the capability to manage with severe channel conditions without complex equalization filters. Chanel equalization is simplified because OFDM may be regarded as many narrowband signals rather than one rapidly modulated wideband signal. The low symbol rate makes the usage of guard interval between symbols rational, making it possible to remove inter-symbol- interference (ISI) and exploit echoes and time-spreading to attain a diversity gain.

However, for mobile applications, channel variations throughout one OFDM symbol cause severe Inter-Carrier-Interference (ICI) which worse the performance of the communication.

OFDM system block architecture can be divided into 3 main components as in Fig.1.1, namely the transmitter, the channel and the receiver. The model used in this thesis is established without the using the Forward Error Correction (FEC) coding (denoted in double-line box).

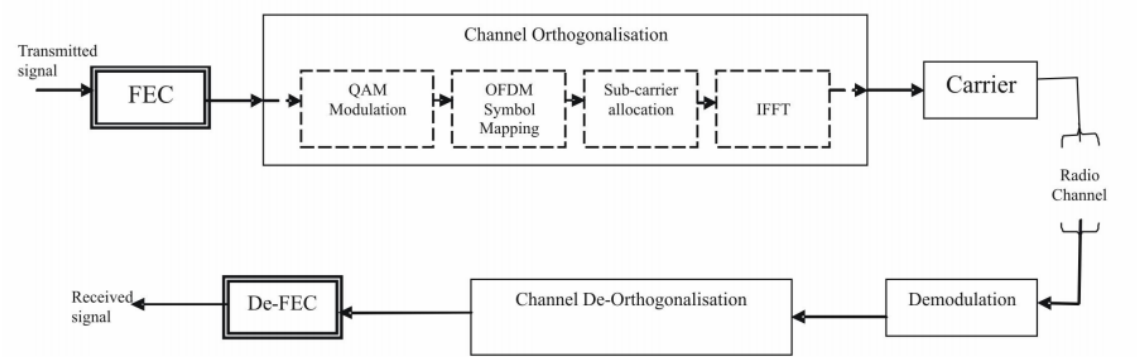

Figure 1.1: Basic Architecture of OFDM system.

1.2 ICI in OFDM due to frequency offset

In a typical wireless communication scenario, the transmitted signal is upconverted to a carrier frequency before broadcast. Upon receiving the signal, the receiver is supposed to adjust to the same carrier frequency to down-convert the signal to baseband before demodulation as shown in Fig.1.2.

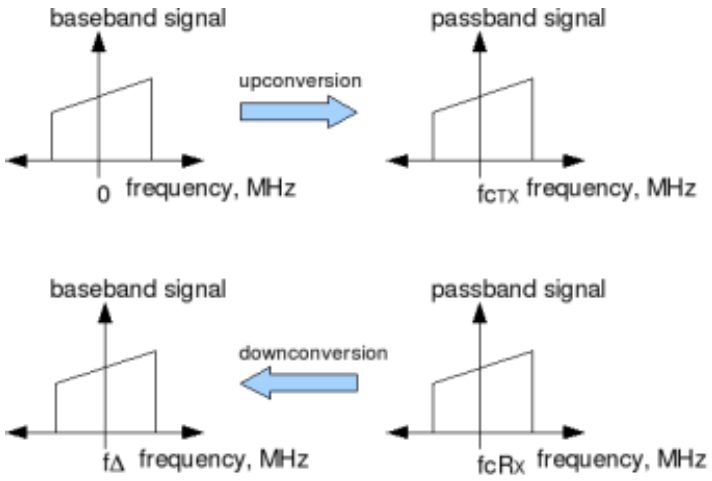

Figure 1.2: Up/down conversion.

However, because of device mismatch or mobility of devices, the carrier frequency of the receiver might not be the same as the carrier frequency of the transmitter. In such case, the received baseband signal, instead of being located at DC (0MHz), will be centered at a certain frequency offset.

Fig.1.3 is the bit error mgnitude as a function of normalized carrier frequency shift in an OFDM communication when the energy per bit to noise power spectral density Eb/N0 equals to 30dB.

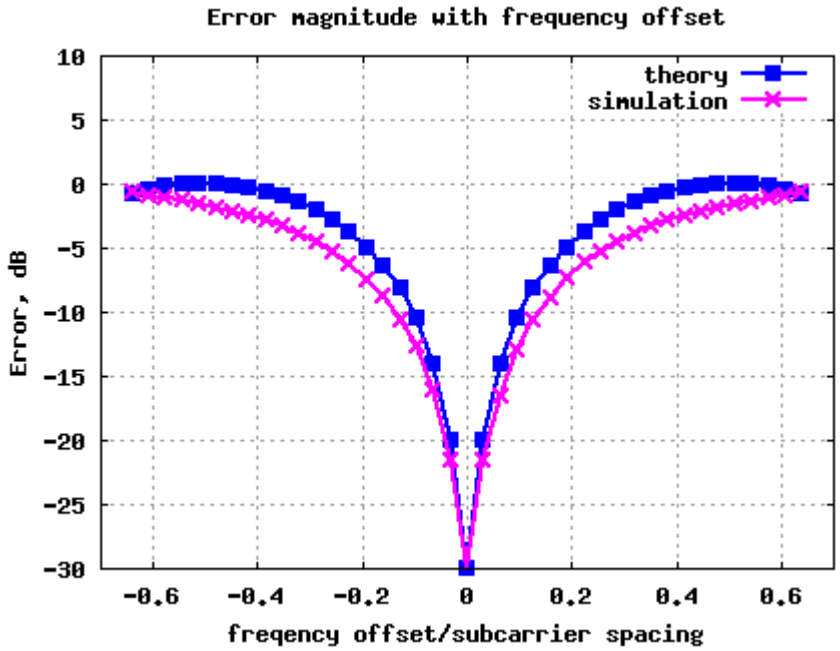

Figure 1.3: Error magnitude versus normalized frequency offset in OFDM.

1.3 ICI mitigation in MIMO-OFDM

Multiple-input multiple-output (MIMO) OFDM systems have arisen as a promising candidate for imminent fourth generation communications due to their high capacity, spectral proficiency, and robustness against fading [4]. Analogous to single-input single-output (SISO) OFDM systems, the carrier frequency offset estimate is a vital difficulty in MIMO OFDM systems. The carrier frequency offset is created by the Doppler shift and/or the incompatibility between transmitter and receiver oscillators. The carrier frequency offset consequences in inter carrier interference, which significantly reduces system performance [5].

The techniques proposed to estimate the carrier frequency offset in SISO OFDM systems can be classified as data-aided methods [6,7] and blind ones [8,9]. However, limited methods can be straightly applied to the much more complex MIMO OFDM systems. Some data-aided methods [10,11] have been suggested for

MIMO OFDM systems. The author of [11] recommended inserting frequency domain training sequences in the signal to estimate the CFO. The cyclic prefix (CP) scheme [12] guesses the carrier frequency offset by examining the cyclic characteristic of the received signal. In general, blind methods are more favorable due to their higher bandwidth efficiency.

1.4 ICI mitigation scheme in HSR MISO-OFDM

With the growth of the High-Speed Railway (HSR), the train velocity can reach up to 350 km/h, or even higher, so more technical requirements for HSR mobile communication system are put forward. Long Term Evolution for Railway (LTE-R) [13] is frequently considered as a promising candidate which can support users with higher data rate and lower latency. Nevertheless, a series of difficulties caused by high movement speed such as over-frequent handover and high Doppler shift need to be answered urgently, and they have become the hot matters in recent years [14]. Particularly in the HSR scenario, time-varying Doppler shifts results in a carrier frequency offset, and degrades the performance of the systems.

1.5 MUSIC algorithm

Smart Antennas are phased array antennas with smart signal processing algorithms used to identify the angle of arrival (AOA) of the signal. This consequently can be used to compute beam-forming vectors needed to detect the intended mobile set. It allows a higher capacity and data rates for all current wireless communications by concentrating the antenna beam on the intended user. Multiple Signal Classification (MUSIC) is a eminent high resolution eigen structure scheme, widely used to estimate the number of signals, and their angles of arrival.

MUSIC algorithm was suggested by Schmidt and his group in 1979 [15]. It has started a new era for spatial spectrum estimation algorithms. The raise of the structure algorithm has become a essential algorithm for theoretical system of spatial spectrum. Before this algorithm was available, many existing related algorithms had directly worked with data received from array covariance matrices. The elementary

idea of MUSIC algorithm is to proceed characteristic decomposition for the output data's covariance matrix, producing in a signal subspace orthogonal with a noise subspace corresponding to the signal. After that, these two orthogonal subspaces are used to establish a spectrum function. Through spectral peak search, the AOA of signal is detected. Since MUSIC algorithm has a high resolution, precision and steadiness under certain conditions, it has drawn a great number of researchers to conduct in-depth researches and analyses. Overall, it has the following benefits when it is used to estimate a signal's AOA:

1) The capability to concurrently measure multiple signals.
2) High precision measurement.
3) High resolution for antenna beam signals.
4) Short data compatibility.
5) Real -time processing based on high-speed processing technology.

In the our project, the MUSIC algorithm is exploited to estimate the carrier frequency offset between RRUs and MS. Although the algorithm is initially used for AOA estimation, MUSIC has been implemented widely in carrier frequency offset estimation because of the similarity in mathematical background.

1.6 Compressed sensing

Compressed sensing is also named as compressive sensing, compressive sampling, or sparse sampling. Compressed sensing is a signal processing technique for proficiently attaining and reconstructing an original signal, by finding solutions to underdetermined linear systems. The algorithm is based on the theory that, through optimization, the sparsity of a signal can be harvested to reconstruct it from far fewer samples than stated by the Shannon-Nyquist sampling theorem. There are two requirements for accurate reconstructing. The first requirement is sparsity which claims that the signal need to be sparse in some domains. The second is incoherence which is applied through the isometric property of represetation of sparse signals.

A mutual objective of engineers in the field of signal processing is to recover original signal from a collection of sampling measurements. General speaking, this problem is not feasible because there is no way to rebuild a signal in the times that the signal is not recorded. However, with prior knowledge or assumptions about the signal, it turns out to be possible to flawlessly reconstruct a signal from a collection of measurements. Throughout history, researchers and engineers have developed their knowledge of which assumptions are pragmatic and how to generalized them.

An early revolution in signal processing was the Nyquist–Shannon sampling theorem. It claims that if the signal's highest frequency is less than half of the sampling rate, the signal can be rebuilt flawlessly. The key idea is that with prior information about the limitations of the signal's frequencies, fewer samples are required to recover the original signal.

In 2004, David Donoho, Emmanuel Candès and Terence Tao showed that provided information about the sparsity of signal, the original signal may be fully recovered with even fewer samples than the Nyquist sampling theorem requires [16]. This concept is the foundation of compressed sensing.

In our application, the channel between each RRU and MS can be considered as sparse in time domain due to the fact that there are only several communicaion paths between RRU and MS. Additionally, in practice, the communication links can be designed such that the line of sight (LOS) component dominate other paths. Based on the sparity of the channel impulse response, we can recover it fully with some known pilot positions of the sending data symbol.

1.7 Subspace clustering

The past few years have seen an innovation in the availability of data from multiple sources and facilities. For instance, millions of cameras have been set in airports, streets, buildings and cities all over the world. This has made extraordinary requirements on how to attain, compress, save, communicate and process enormous amounts of complex high-dimensional data. Many of these methods depended on the

observation that, although these data sets are high-dimensional, their intrinsic dimension is commonly much smaller than the dimension of the ambient space. For example in computer vision, the number of pixels in an image can be very large, however most computer vision models rely only on several parameters to depict the appearance, structure and dynamics of a scene. This has inspired the development of several methods for searching a low-dimensional representation of a high-dimensional data set. Traditional techniques, such as Principal Component Analysis, makes the assumption that the data is extracted from a single low-dimensional subspace of a high-dimensional space. Such approaches have instigated many applications in a lot of fields.

Practically, however, the data points could be originated from multiple subspaces and the membership of the data points to the subspaces might be unidentified. For instance, a video sequence could comprise several moving objects and different subspaces might be required to define the motion of different objects in the movie section. Thus, there is a necessity to concurrently group the data into multiple subspaces and detect a low-dimensional subspace for each group of data. This problem, known as subspace clustering, has formed a lot applications in many fields, e.g., image processing, pattern recognition, bioinformatics, data compression, etc. [17].

1.8 Chaotic mapping

Mathematically, a chaotic map is a map that has some sort of chaotic behavior. Map may be parameterized by a discrete-time or continuous-time parameter. Discrete maps frequently take the form of iterated functions.

In our development of OFDM system using chaotic mapping, we apply the Discrete Baker Mapping (DBM) as our coding algorithm. The Baker's map is a chaotic map from the unit square into itself. It is named after a kneading operation that bakers apply to dough: the dough is cut in half, and the two halves are staked on the one another, and compressed.

The chaotic Baker map is implemented to randomize subcarrier; as a result, adds a degree of encryption to the transmitted data.

1.9 Purposes of project

In this project we focus on estimating carrier frequency shift as well as channel in OFDM communication system. The detailed goals are listed in Table 1.1.

Table 1.1: Project objectives.

	Objectives	Status
1	Estimation of single CFO in HSR SISO OFDM	Done
2	Estimation of double CFO in HSR MISO OFDM	Done
3	Channel estimation in HSR conventional OFDM based on compressed sensing	Done
4	Channel estimation in HSR conventional OFDM based on compressed sensing and manifold	On going
5	Chaotic subcarriers interleaving	Done

1.10 Related work

ICI mitigation in OFDM

In the single-input single-output (SISO) or the co-located multi-input multi-output (MIMO) OFDM systems, there is only one CFO between the transceivers, where a lot of researches on CFO approximation have been carried out with both data-aided approach and blind approach [6-12]. On the other side, when distributed transmitters transmit data streams at the same time, multiple CFOs will be obtained at the receiver, making the CFO approximation and compensation more perplexing. A well-known scenario is the so-called orthogonal frequency division multiple access (OFDMA), in which the subcarriers are completely occupied by the many users. Throughout the past few years, several multiuser CFO estimation techniques for OFDMA uplink have been proposed [18,19], where different CFOs could either be estimated from an iterative methods or be detected from some subspace schemes.

With the growing need of improving spectral utilization, the multiuser uplink transmissions with spatially multiplexed (SM) OFDM have gained significant consideration. In this condition, one subcarrier could be concurrently occupied by multiple users and thus a much higher spectral efficiency can be accomplished. Nevertheless, multiple users occupying the same subcarrier makes the CFO estimation more challenging. There are very few researches on multiple CFO estimation for multiuser OFDM transmission. Besson and Stoica made the first trial in [20] while limited their simultion only for flat fading channels. In [21], a semi-blind scheme was suggested to instantaneously approximate the multiple CFOs and channels in frequency selective fading channels; however, the technique is only effective for zero-padding (ZP) OFDM, as ZP can make the channel estimation and equalization more simple. A joint CFO and channel estimation for multiuser cyclic-prefix (CP) MIMO-OFDM systems was introduced in [22] based on the maximum likelihood (ML) criterion. The high-complex multi-dimensional search is reduced from the importance sampling technique, however the remaining complexity to create sufficient samples for importance sampling may still be large for real application

implementation. A suboptimal estimation algorithm was presented in [23]. More recently, the authors of [24] introduced a semiblind multi-CFO approximation and an independent component analysis based equalization scheme for multiuser coordinated multi-point OFDM systems.

In this thesis, the problem of double CFOs is investigated. The contributions of this thesis is the estimation of CFOs with only one received antenna (rather than many antennas as shown in [20-24]) without the implement of training sequence as in [24]. As a result, we do not need the assumption that the channel among trasmittersand receiver antennas are uncorrelated. We also show that our proposed method out perform the conventional estimation method in [25] at high SNR.

Compressed sensing channel estimation

Lately, there has been a rising attention in compressed sensing (CS) [26-28], which has been broadly applied in many areas such as image processing, communication systems, and so on. Based on CS theory, when a signal possesses a sparse representation in a certain space, one can record the signal at a rate significantly lower than the Nyquist rate and recover it with high accuracy with optimization techniques. The fundamental of pilot-assisted channel estimation in OFDM systems is to rebuild the channel frequency responses for all the subcarriers from those acquired on the pilot subcarriers. The number of pilot symbols implemented in traditional pilot-assisted channel estimation techniques is large since it is set by the Nyquist sampling theorem. By applying the CS theory and exploiting the sparsity of the channel, it is possible that the number of pilot symbols can be reduced [29-31]. In [29,31] the CS chanel estimation has been applied for sparse channel impulse responses in multicarrier systems.

In this thesis, we proposed a research direction which rely on the theory of compressed sensing and subspace clustering to further estimate the channel information.

Chaotic subcarriers interleaving

In recent years, both ODFM and chaotic algorithms have been widely developed for wideband digital communication systems [32-39]. There are various chaotic communications system have been proposed: chaotic modulation, chaotic masking, chaos shift keying and its variants, etc [35-37]. In our investigation, we focus on applying DBM on subcarriers in OFDM. As discussed in [33, 35 ,39], various researchers proposing OFDM systems using chaotic algorithms. However, those systems have showed several drawbacks. For instance, applying DBM in input bits [33, 39] introduces considerable delay since those bits are required to be buffered before S/P step. Or as in [35], chaotic encryption systems might have higher BER than conventional systems.

1.11 Research methodology

The OFDM communication system is modeled by MATLAB using Monte Carlo simulation. The simulation results are compared with results of other recent researches.

CHAPTER 2

CARRIER FREQUENCY OFFSETS ESTIMATION IN HSR OFDM

In this chapter, theoritical background, system model and simulation results of ICI mitigation based on MUSIC algorithm are examined.

2.1. OFDM with single Carrier frequency offset

The block model of conventional OFDM architecture is demonstrated in Fig.2.1. In the transmitter, the data is initially put into the serial-to-parallel block, in which the input data stream is separated into N sub-stream with N time lower data rate. Then, by applying inverse Discrete Fourier transform block on the N-input OFDM symbol, we get the time domain signal for transmission. Before converting the signal to analogue, guard interval is appended to lessen the effect of inter-symbol-interference due to long symbol duration.

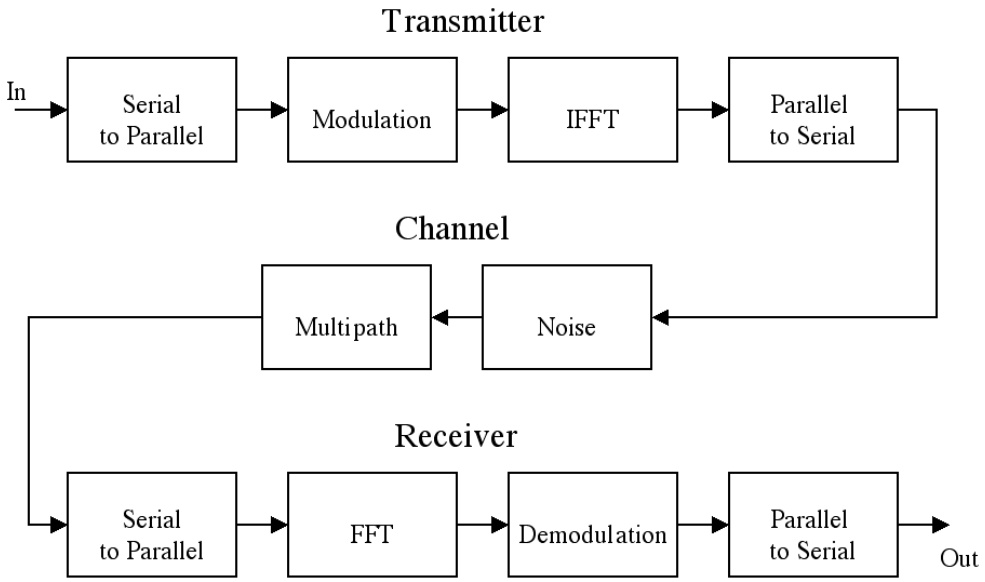

Figure 2.1: Conventional OFDM system.

At the receiver, the inverse processes are applied. At the first step, the signal is converted to digital. The guard interval is then detached and the Discrete Fourier Transform is performed to transform the signal into parallel OFDM symbols. The

final step is serializing the symbols into data stream. In OFDM, multiple sinusoidal with frequency separation 1/ T_s is used where T_s is the symbol duration. Denote:

N: $Number\ of\ subcarriers$.

P: $Number\ of\ slots\ for\ data\ in\ N\ subcarriers\ (P < N)$.

$s(k)$: $k^{th} OFDM\ symbol \rightarrow s(k) = [s_1(k)\ s_2(k)\ ...\ s_P(k)]^T$. (2.1)

The OFDM modulation is performed by applying an inverse-DFT (IDFT) operator to the data stream. Using matrix representation, the resulting N-point time domain signal is given by:

$$x(k) = [x_1(k)\ x_2(k)\ ...\ x_N(k)]^T = \boldsymbol{W}_P s(k), \quad (2.2)$$

where $\boldsymbol{W}_P$ is a first P column of the $N \times N$ IDFT matrix $\boldsymbol{W}$:

$$\boldsymbol{W} = IDFT(N) = [w_1\ ...\ w_N]. \quad (2.3)$$

$$\boldsymbol{W}_P = [w_1\ ...\ w_P]. \quad (2.4)$$

Practically, to prevent transmit filtering in OFDM system, some subcarriers are not modulated. In other words, the number of subchannels carrying the information is generally smaller than the size of the DFT block. Without adjacent-channel-interference, the outputs from these virtual carriers are zero. Without loss of generality, we assume carriers from 1 to P are used for data transmission so that we have equation (2.4). In discrete Fourier transform (DFT)-based OFDM, a cyclic prefix (CP) is added to the multiplexed output of the IDFT before it is transmitted through a fading channel [40]. After that, the CP is detached at the receiver. Here, we do not put it into equation.

Denote:

$\boldsymbol{h}$: $Channel\ impulse\ response$.

$$[H(1)\ ...\ H(N)] = FFT(\boldsymbol{h})\ (N - point\ FFT\ of\ \boldsymbol{h}). \quad (2.5)$$

$$\boldsymbol{H} = diag[H(1)\ ...\ H(N)]. \quad (2.6)$$

$$\boldsymbol{H_P} = diag[H(1)\ ...\ H(P)]. \quad (2.7)$$

The receiver input for the k-th block without noise and CFO is given by:

$$y(k) = \boldsymbol{h}\boldsymbol{W}_P s(k) = \boldsymbol{W}_P \boldsymbol{H}_{\boldsymbol{P}} s(k). \quad (2.8)$$

It is clear that, each subchannel, with a scalar ambiguity, can be recovered by applying a DFT to $y(k)$:

$$\boldsymbol{W}_P^H y(k) = \boldsymbol{H}_{\boldsymbol{P}} s(k). \quad (2.9)$$

Denote φ the normailized carrier frequency offset and Ng the guard interval duration of OFDM symbol. In the presence of a carrier offset, $e^{j\varphi}$, the receiver input $y(k)$ without noise is modulated by:

$$\boldsymbol{E}(\varphi) = diag[\,1, e^{j\varphi}, e^{j2\varphi}, \dots, e^{j(N-1)\varphi}], \quad (2.10)$$

and becomes:

$$y(k) = \boldsymbol{E}(\varphi)\boldsymbol{W}_P \boldsymbol{H}_{\boldsymbol{P}} s(k) e^{j(k-1)(N+Ng)\varphi}. \quad (2.11)$$

Since $\boldsymbol{W}_P^H \boldsymbol{E}(\varphi)\boldsymbol{W}_P \neq \boldsymbol{I}$, the $\boldsymbol{E}(\varphi)$ matrix breaks the orthorgonality among the subchannels and, as a result, introduces ICI. To recover $s(k)$, the carrier offset, φ , requires to be estimated and compensated before applying the DFT.

2.2. System model

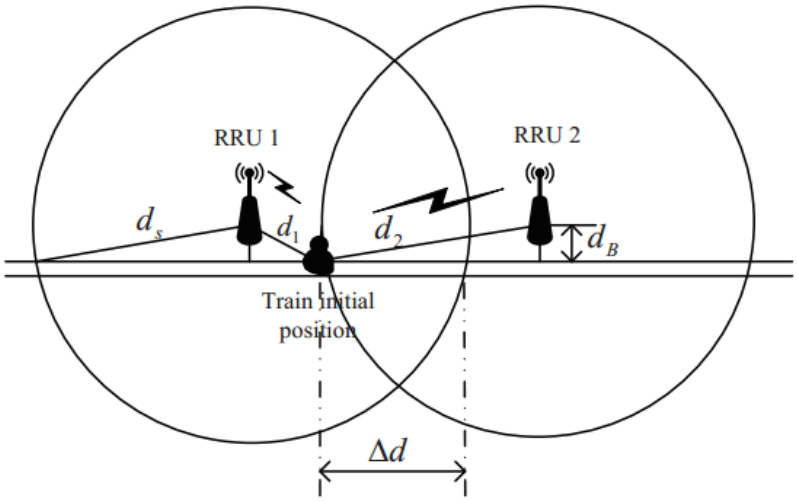

Figure 2.2: Communication scenario for HSR MISO-OFDM.

The HSR system we study is a two-hoop network structure formed by distributed RRUs as illustrated in Fig.2.2. Here we primarily examine the communication of RRU-MS links. Each RRU can be designed with one or more antennas. We make the assumption that the coverage region of each RRU forms a logic cell, and each RRU has one antenna and the MS also has one antenna. All the antennas have no correlation with each other. The Doppler frequency shifts are our main research objective, so we assume the system has been synchronized in time and oscillator frequency.

In our simulation, we assign time-frequency resource to the two adjacent RRUs just as the two-TX scenario in downlink system in [41]. Desired signals from the two RRUs reach the MS almost instantaneously. The two signal streams cannot be detached easily because they occupy the same time-frequency slot in the OFDM communication link. Consequently, it is still problematic to compensate Doppler frequency offsets precisely at the receiver. A proposed solution is given as in Fig.2.3 The MS estimates Doppler frequency shifts based on the received data and then feeds the estimated value back to RRU. When the new data is sent, the frequency offset pre-compensation is made for the data. It is worth to note that prediction according

to variation of Doppler frequency shift is also possible to further enhance the effect of pre-compensation. We also have to point out that error would be presented because of the feedback delay produced by the fast time-varying channel.

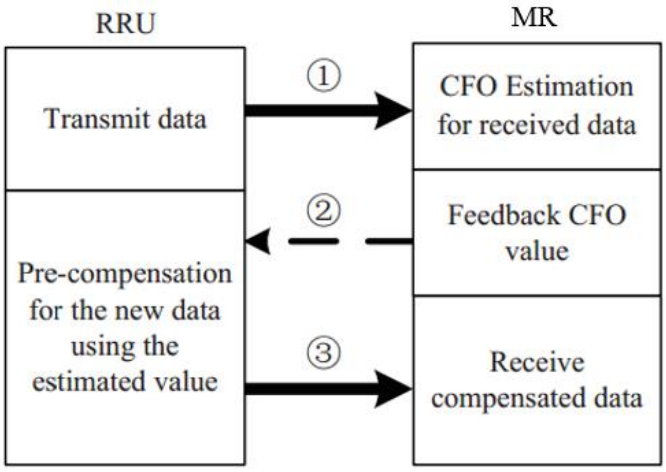

Figure 2.3: The pre-compensation scheme.

As in Fig.2.2, we can see that the received signal is the mixture of two signals from two seperated RRUs. As the MS was moving away from RRU1 and toward RRU2 , the Doppler frequency shift of these two signals were undoubtedly different. In this project, through mathematical models of channel and communication scenarios, we found out the two frequency shifts based on a preamble frame of data in communication link between RRUs and MS. This method is an improvement of MUSIC algorithm in [3].

2.3. Generation of carrier frequency offset

In the HSR OFDM, we model the Doppler shift as:

$$f_p(t) = f_d cos\theta(t) = f_c \frac{v}{c} cos\theta(t), \tag{2.12}$$

where $f_p(t)$ denotes the Dopper shift. f_d is the maximum Doppler frequency; f_c is carrier frequency; v is the velocity of MS and c is the speed of light. The angle of arrival $cos\theta(t)$ is given by:

$$cos\theta(t) = \frac{d_s - vt}{\sqrt{d_B^2 + (d_s - vt)^2}}, 0 \le t \le 2d_s/v, \quad (2.13)$$

where t is programmed when the train move into the cell; d_s is the coverage radius of one RRU and d_B is the perpendicular distance between RRU and railway (as shown in Fig.4). Subsequently, the normalized frequency offset is given by:

$$\varphi(t) = f_p(t)\frac{N}{f_{sample}}, \quad (2.14)$$

where f_{sample} is the sampling frequency.

2.4. Estimation of single Carrier frequency offset

Since $\boldsymbol{W}_P$ contains of a subset of the columns of the IDFT matrix, $\boldsymbol{W}$, its orthogonal complement, $\boldsymbol{W}^{\perp} = [w_{P+1} \dots w_N]$, is known. Thus, in the absence of the carrier offset ($\varphi = 0$), we have:

$$w_{p+i}{}^H y(k) = w_{p+i}{}^H \boldsymbol{W}_P \boldsymbol{H_P} s(k) = 0, \qquad (i = 1, \dots, N-P). \quad (2.15)$$

This is not true when $\varphi \neq 0$. However, if we let

$$\boldsymbol{Z}(\omega) = diag[\,1, e^{j\omega}, e^{j2\omega}, \dots, e^{j(N-1)\omega}]. \quad (2.16)$$

It can be shown that when $\omega = \varphi$ or $\boldsymbol{Z}(\omega) = \boldsymbol{E}(\varphi)$:

$$\begin{aligned} & w_{p+i}{}^H \boldsymbol{Z}(\omega)^{-1} y(k) \\ &= w_{p+i}{}^H \boldsymbol{Z}(\omega)^{-1} \boldsymbol{E}(\varphi) \boldsymbol{W}_P \boldsymbol{H_P} s(k) e^{j(k-1)(N+Ng)\varphi} \\ &= 0, \quad (i = 1, \dots, N-P). \end{aligned} \quad (2.17)$$

This observation suggests that we form a cost function based on a finite number of data vectors as follows:

$$\begin{aligned} P(\omega) &= \sum_{k=1}^{K} \sum_{i=1}^{N-P} ||w_{p+i}{}^H \boldsymbol{Z}(\omega)^{-1} y(k)||^2 \\ &= \sum_{k=1}^{K} \sum_{i=1}^{N-P} w_{p+i}{}^H \boldsymbol{Z}(\omega)^{-1} y(k) y^H(k)\, \boldsymbol{Z}(\omega) w_{P+i}, \end{aligned} \quad (2.18)$$

where K is the number of symbols in one frame.

Clearly, $P(\omega)$ is zero when $\boldsymbol{Z}(\omega) = \boldsymbol{E}(\varphi)$. Therefore, one can find the carrier offset by evaluating $P(\omega)$ along the unit circle.

The proposed algorithm is summarized in the following:

1) Form the cost function as in (2.18) using the receiver outputs $y(k)$.
2) Estimate the carrier offset as the null of $P(\omega)$ or the phase of the root of $P(\boldsymbol{Z}(\omega))$. In the presence of noise, the carrier offset is estimated as the minima of $P(\omega)$:

$$\hat{\varphi} = \omega_0 : P(\omega_0) = min\ P(\omega). \quad (2.19)$$

2.5. Simulation of Single Carrier frequency offset estimation

Simulations were performed to illustrate the proposed algorithm. We use the parameters shown in Table 2.1 to establish the communication scenario.

Table 2.1: Simulation parameters for Single CFO estimation.

Parameters	Values
Cell radius (ds)	500 m
Travel region (Δd)	400 m
Initial distance between train and RRU (d)	100 m
Distance between railway and RRUs (dB)	50 m
Velocity of train (v)	360 km/h
Subcarrier spacing (Δf)	60-120 kHz
Bandwidth (BW)	10 MHz
Sampling Frequency (fs)	15.36 MHz
Total number of subcarriers (N)	128 and 256
Modulation	BPSK

Fig 2.4 shown the CFO of communication link when the MS was going far away from RRU. As the train was moving, the absolute value of CFO increased. As we can see from the figure, the algorithm was not accurated at low SNR. However, only at 15 and 20dB, it shown little differet with actual value. Fig 2.5 illustrates the peak of the inverse of cost function $P(\omega)$ at SNR=25dB and normalized CFO= 0.001. Lastly, the mean square error of the MUSIC based estimation is shown in Fig 2.6. The similar result can be found in [3].

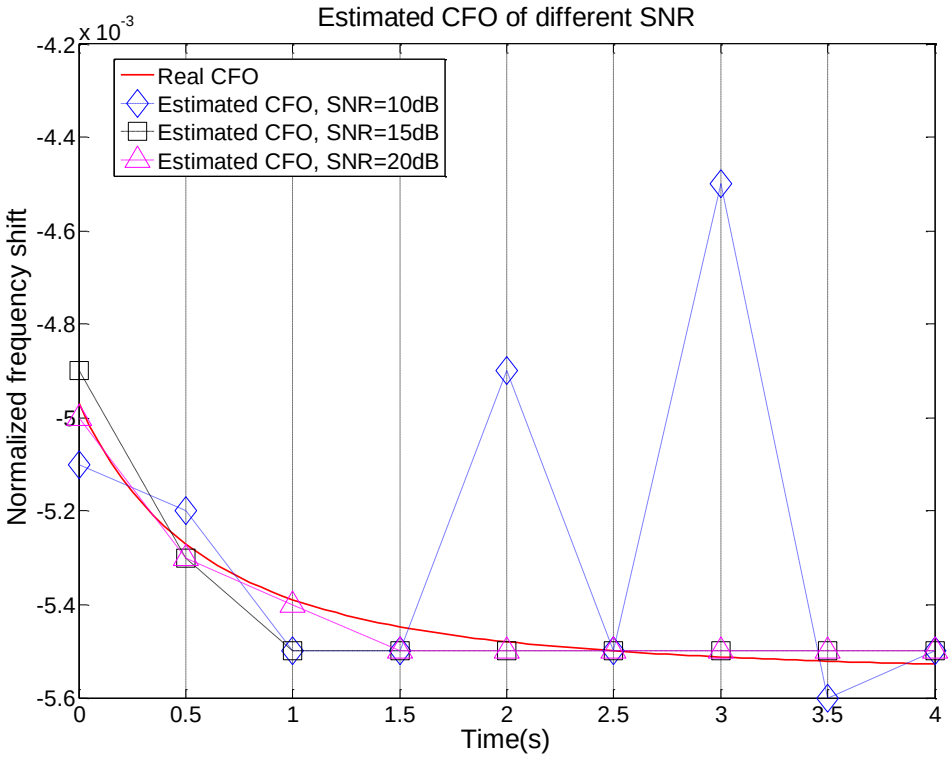

Figure 2.4: The estimated CFO and the actual CFO.

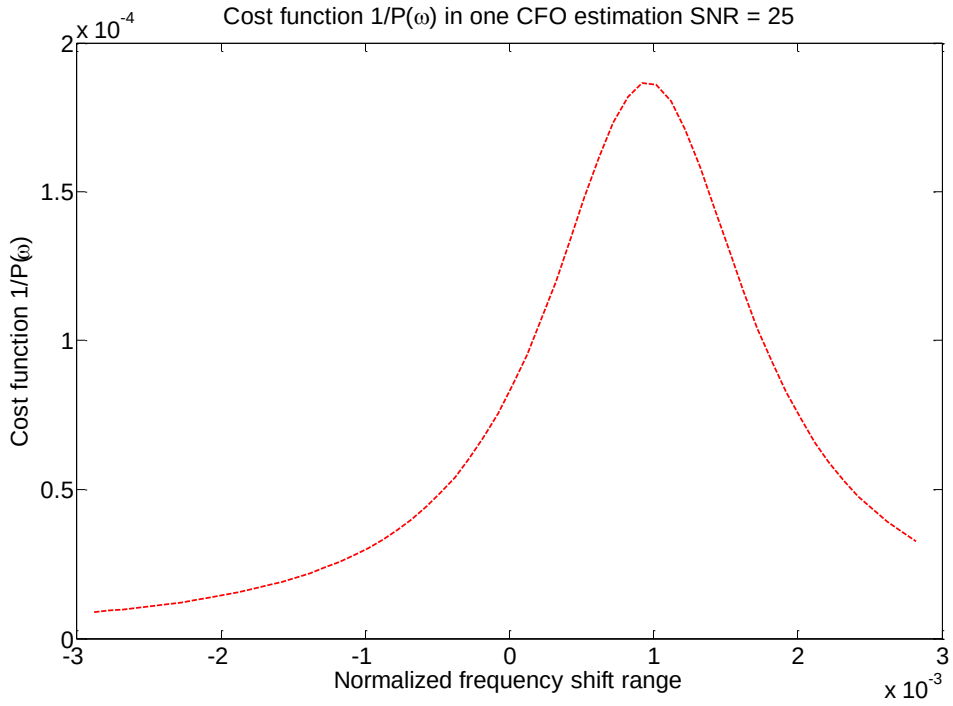

Figure 2.5: The inverse cost function when CFO=0.001 and SNR=25dB.

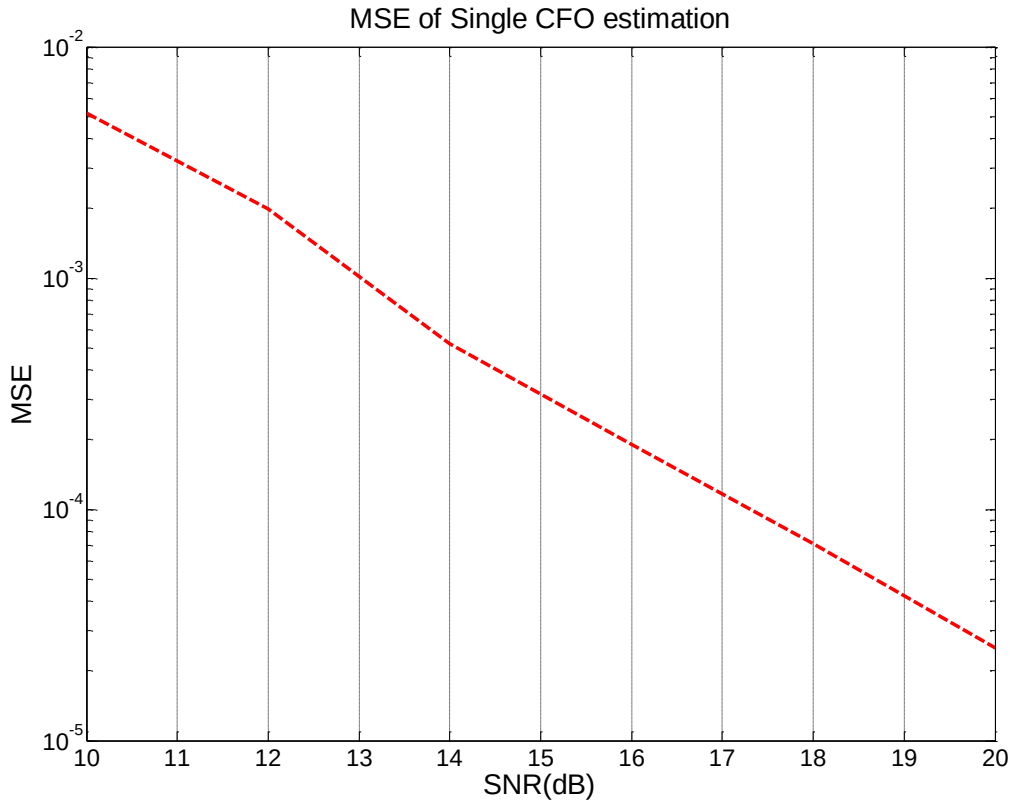

Figure 2.6: MSE of MUSIC based CFO estimation.

2.6. OFDM with double Carrier frequency offsets

In case if HSR-OFDM, the received signal is the combination of signals from two sources. From equation (2.11), we have the received signal from one transmitter without noise is:

$$y1(k) = \boldsymbol{E}(\varphi_1)\boldsymbol{W}_P\boldsymbol{H_{1P}}s(k)e^{j(k-1)(N+Ng)\varphi}. \quad (2.20)$$

where φ_1 is the normalized carrier frequency shift from the first RRU and $\boldsymbol{H_{1P}}$ is the channel frequecy response matrix similar to $\boldsymbol{H_P}$. With K is the number of OFDM symbols in one frame, we have one frame of received signal from one RRU is:

$$\boldsymbol{y1} = \boldsymbol{E}(\varphi_1)\boldsymbol{W}_P\boldsymbol{H_{1P}}\boldsymbol{s}^T\boldsymbol{B}(\varphi_1). \quad (2.21)$$

Where $\boldsymbol{s} = [s(1), s(2), \dots s(K)]^T$ is the sending data in one frame and $\boldsymbol{B}(\varphi) = diag\left[1, e^{j(N+Ng)\varphi}, e^{j2(N+Ng)\varphi}, \dots, e^{j(K-1)(N+Ng)\varphi}\right]$ is the carrier frequency offset matrix along OFDM symbols.

With 2 RRUs, the received data frame without noise is:

$$\boldsymbol{y} = \boldsymbol{E}(\varphi_1)\boldsymbol{W}_P\boldsymbol{H_{1P}}\boldsymbol{s}^T\boldsymbol{B}(\varphi_1) + \boldsymbol{E}(\varphi_2)\boldsymbol{W}_P\boldsymbol{H_{2P}}\boldsymbol{s}^T\boldsymbol{B}(\varphi_2). \quad (2.22)$$

Similar to the case of single carrier frequency offset, to recover $s(k)$, the carrier offsets, $\varphi_1$and φ_2 , need to be estimated and compensated before performing the DFT.

2.7. Estimation of double Carrier frequency offsets

Considering a preamble data frame in which $\boldsymbol{s}$ is known in prior. Let the number of symbols per frame K greater than the number of data slots P, we construct $\dot{\boldsymbol{s}}$ from $\boldsymbol{s}$ as follow:

1) Singular value decomposing $\boldsymbol{s^T}$ into $\boldsymbol{U}, \boldsymbol{D}, \boldsymbol{V}$:

$$\boldsymbol{s^T} = \boldsymbol{UDV}, \quad (2.23)$$

in which $\boldsymbol{U}$ and $\boldsymbol{V}$ are $P \times P$ and $K \times K$ unitary matrix respectively. $\boldsymbol{D}$ is a rectangular diagonal matrix with non-negative real numbers on the diagonal.

2) $\dot{\boldsymbol{s}}$ is the last K-P column of the $K \times K$ matrix $\boldsymbol{V}$:

$$\dot{\boldsymbol{s}} = [v_{K-P+1}, \dots, v_K] = [\dot{s}_1, \dot{s}_2, \dots, \dot{s}_{K-P}]. \quad (2.23)$$

Consequently, we have:

$$\boldsymbol{s^T}\dot{s}_k = null\ vector. \quad (2.24)$$

Denote:

$$\boldsymbol{T}(\omega) = diag\big[\,1, e^{j(N+Ng)\omega}, e^{j2(N+Ng)\omega}, \dots, e^{j(K-1)(N+Ng)\omega}\big]. \quad (2.25)$$

In the absensce of noise, if $\omega_1 = \varphi_1$ and $\omega_2 = \varphi_2$, we have:

$$\begin{aligned}
&{w_{p+i}}^H \boldsymbol{Z}(\omega_1)^{-\mathbf{1}} \boldsymbol{y}\, \boldsymbol{T}(\omega_2)^{-\mathbf{1}} \dot{s}_k \\
&= {w_{p+i}}^H \boldsymbol{Z}(\omega_1)^{-\mathbf{1}} \big\{ \boldsymbol{E}(\varphi_1)\boldsymbol{W}_P \boldsymbol{H_{1_P}} \boldsymbol{s}^T \boldsymbol{B}(\varphi_1) \\
&\qquad + \boldsymbol{E}(\varphi_2)\boldsymbol{W}_P \boldsymbol{H_{2_P}} \boldsymbol{s}^T \boldsymbol{B}(\varphi_2) \big\} \boldsymbol{T}(\omega_2)^{-\mathbf{1}} \dot{s}_k \\
&= {w_{p+i}}^H \boldsymbol{Z}(\omega_1)^{-\mathbf{1}} \boldsymbol{E}(\varphi_1)\boldsymbol{W}_P \boldsymbol{H_{1_P}} \boldsymbol{s}^T \boldsymbol{B}(\varphi_1)\, \boldsymbol{T}(\omega_2)^{-\mathbf{1}} \dot{s}_k \\
&\qquad + {w_{p+i}}^H \boldsymbol{Z}(\omega_1)^{-\mathbf{1}} \boldsymbol{E}(\varphi_2)\boldsymbol{W}_P \boldsymbol{H_{2_P}} \boldsymbol{s}^T \boldsymbol{B}(\varphi_2)\, \boldsymbol{T}(\omega_2)^{-\mathbf{1}} \dot{s}_k \\
&= 0, (i = 1, \dots, N-P; k = 1, \dots, K-P).
\end{aligned} \quad (2.26)$$

This observation suggests that we form a cost function given a finite number of data vectors as follows:

$$\begin{aligned}
&P(\omega_1, \omega_2) = \sum_{k=1}^{K-P} \sum_{i=1}^{N-P} \left| {w_{p+i}}^H \boldsymbol{Z}(\omega_1)^{-\mathbf{1}} \boldsymbol{y}\ \boldsymbol{T}(\omega_2)^{-\mathbf{1}} \dot{s}_k \right|^2 = \\
&\sum_{k=1}^{K-P} \sum_{i=1}^{N-P} {w_{p+i}}^H \boldsymbol{Z}(\omega_1)^{-\mathbf{1}} \boldsymbol{y}\ \boldsymbol{T}(\omega_2)^{-\mathbf{1}} \dot{s}_k \dot{s}_k{}^H \boldsymbol{T}(\omega_2) \boldsymbol{y}^H \boldsymbol{Z}(\omega_1) w_{p+i}.
\end{aligned} \quad (2.27)$$

Clearly, $P(\omega_1, \omega_2)$ is zero when $\omega_1 = \varphi_1$ and $\omega_2 = \varphi_2$. Therefore, one can find the carrier offsets by evaluating $P(\omega_1, \omega_2)$ along the two independent unit circles. However, we can see that the cost function also has root $\omega_1 = \varphi_2$ and $\omega_2 = \varphi_1$; hence, the cost function has two minimas. Fig.2.7 is the inverse cost function with

N=128, SNR = 25dB, $\varphi_1 = 0.0055$ and $\varphi_1 = -0.0042$. The surface has two peaks as we predicted.

Due to the fact that the we have to solutions in the form (φ_1, φ_2) and (φ_2, φ_1); we proposed finding maxima of the following symmetric cost function to further enhance the performance:

$$\boldsymbol{Q}(\omega_1, \omega_2) = P(\omega_1, \omega_2) + P(\omega_2, \omega_1). \quad (2.28)$$

Fig.2.8 is the inverse of $\boldsymbol{Q}(\omega_1, \omega_2)$ with N=128, SNR = 25dB, $\varphi_1 = 0.0055$ and $\varphi_1 = -0.0042$. The surface also has two peaks as in Fig.2.4; however, they are much more visible.

The proposed algorithm is summarized in the following:

1) Form the cost function $\boldsymbol{Q}(\omega_1, \omega_2)$ as in (2.27) and (2.28) using the known preamble data $\boldsymbol{s}$ and the receiver outputs $\boldsymbol{y}$.
2) Estimate the carrier offset as the minima of $\boldsymbol{Q}(\omega_1, \omega_2)$:

$$(\hat{\varphi}_1, \hat{\varphi}_2) = (\omega_{0_1}, \omega_{0_2}): \boldsymbol{Q}(\omega_{0_1}, \omega_{0_2}) = min\ \boldsymbol{Q}(\omega_1, \omega_2). \quad (2.29)$$

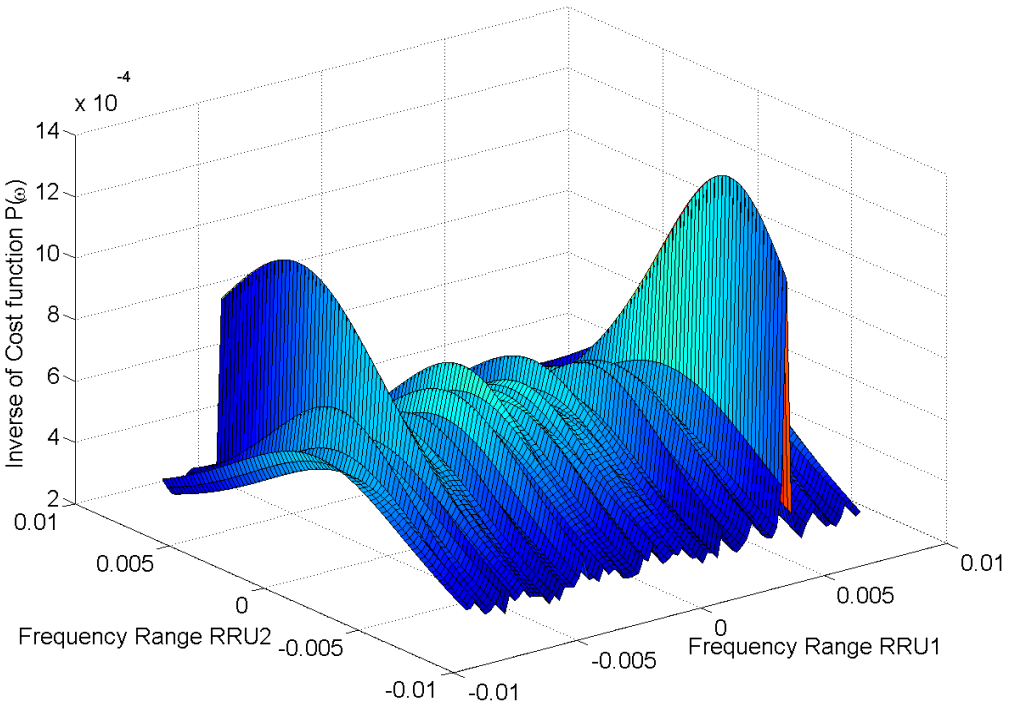

Figure 2.7: The inverse cost function of double CFOs estimation.

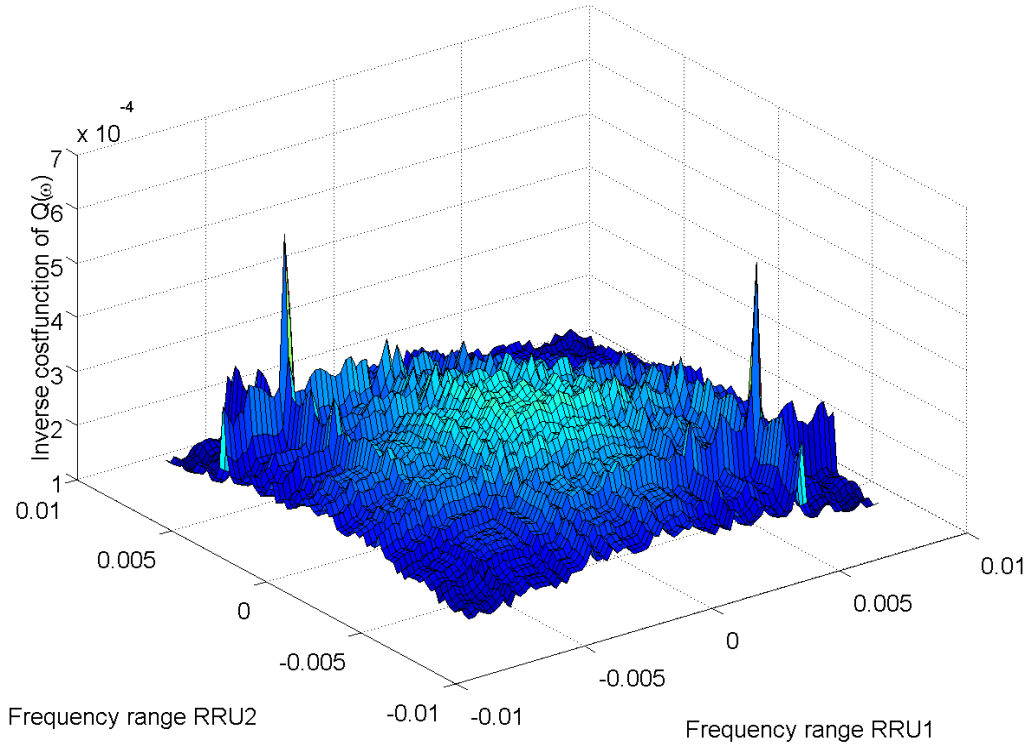

Figure 2.8: The inverse symmetric cost function of double CFOs estimation.

2.8. Simulation of Double Carrier frequency offset estimation

We use the parameters shown in Table 2.2 to establish the communication scenario. In the simulation, we focus on the two communication links between RRUs and MS. We assume that the system has already achive the signal time synchronization at the receiver.

Table 2.2: Simulation parameters for Double CFO estimation.

Parameters	Values
Cell radius (ds)	500 m
Overlap coverage region (Δd)	400 m
Initial distance between train and RRU1 (d1)	100 m
Initial distance between train and RRU2 (d2)	400 m
Distance between railway and RRUs (dB)	50 m
Velocity of train (v)	360 km/h
Subcarrier spacing (Δf)	120 kHz
Bandwidth (BW)	10 MHz
Sampling Frequency (fs)	15.36 MHz
Total number of subcarriers (N)	128
Modulation	BPSK

Fig.2.9 and Fig.2.10 shown the CFO of communication links when the MS was going far away from RRU1 and toward RRU2. Similar with Single CFO estimation, the proposed algorithm was not accurated at low SNR. However, it achieves high accuracy at higher SNR.

The accuracy of our proposed method is described in Fig.2.10. Here, we compare our proposed method with the conventional solution as shown in [25]. At higher SNR, our algorithm has shown its dominance.

Fig 2.11 is the BER of our communication scheme compare with communication link with no CFO and communication linh with CFO but no CFO compensation. As SNR got higher, our algorithim results approached the real CFO value; hence, the performance got closer to ideal case.

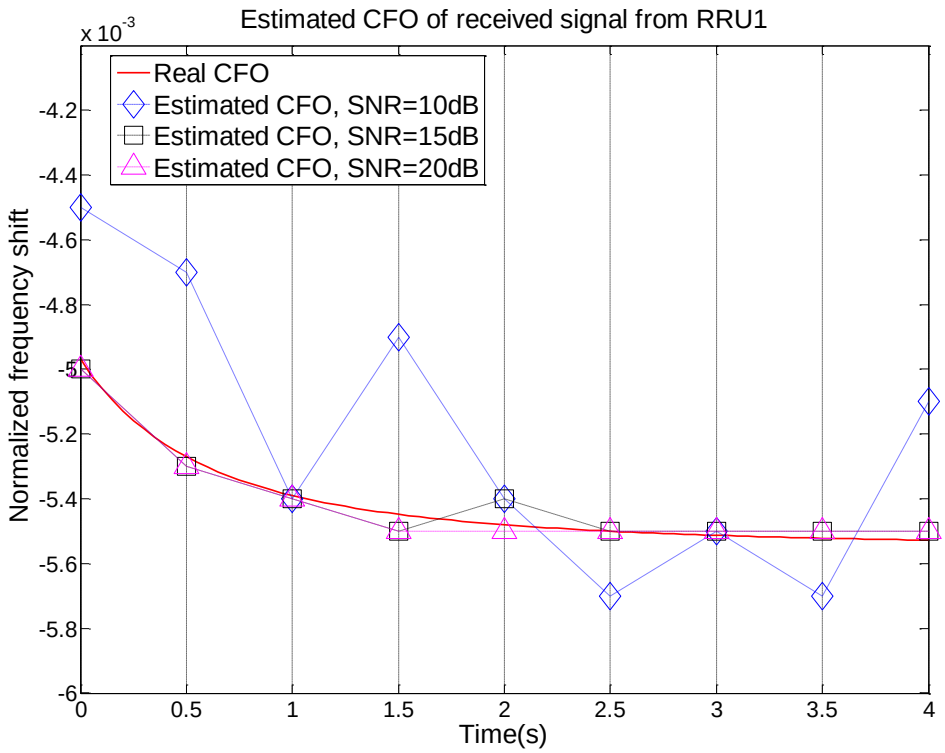

Figure 2.9: The estimated CFO and the actual CFO at RRU1.

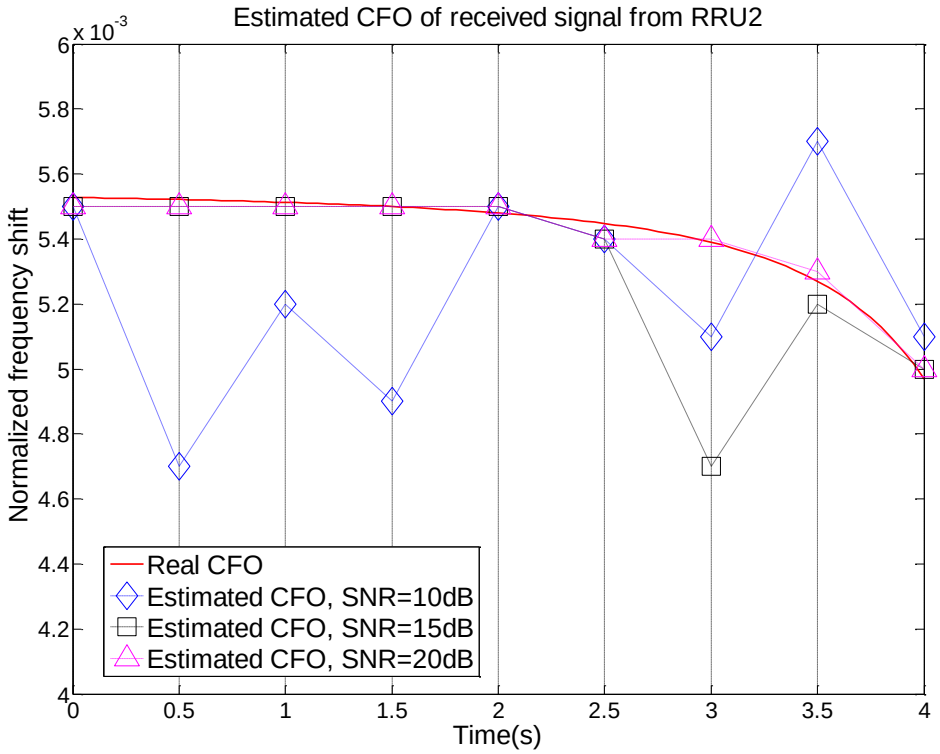

Figure 2.10: The estimated CFO and the actual CFO at RRU2.

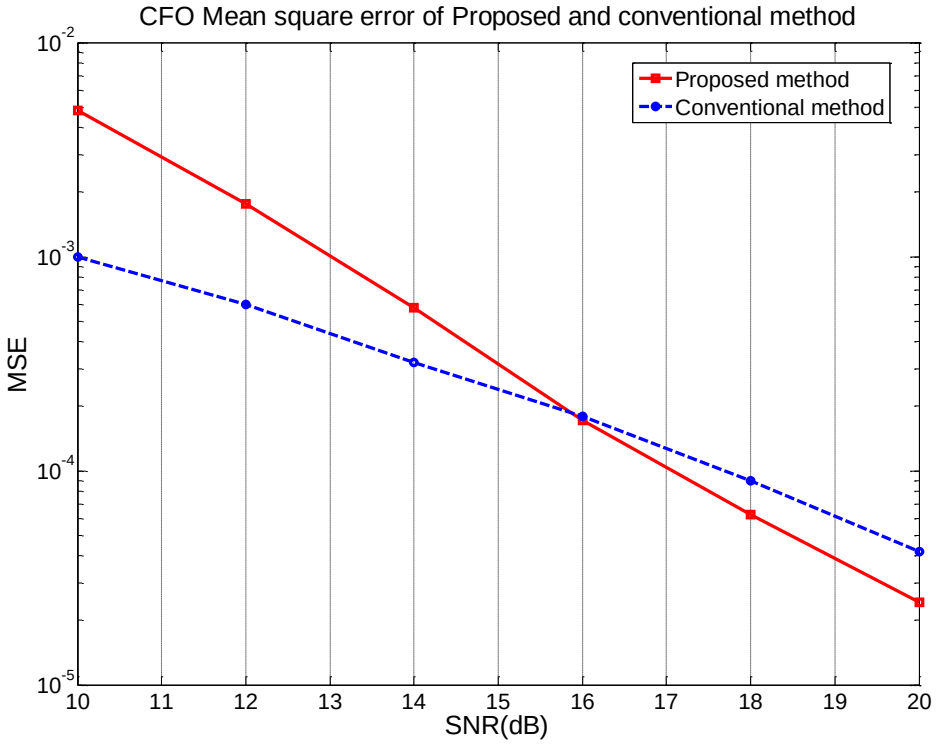

Figure 2.11: MSE of the proposed algorithm and conventional method.

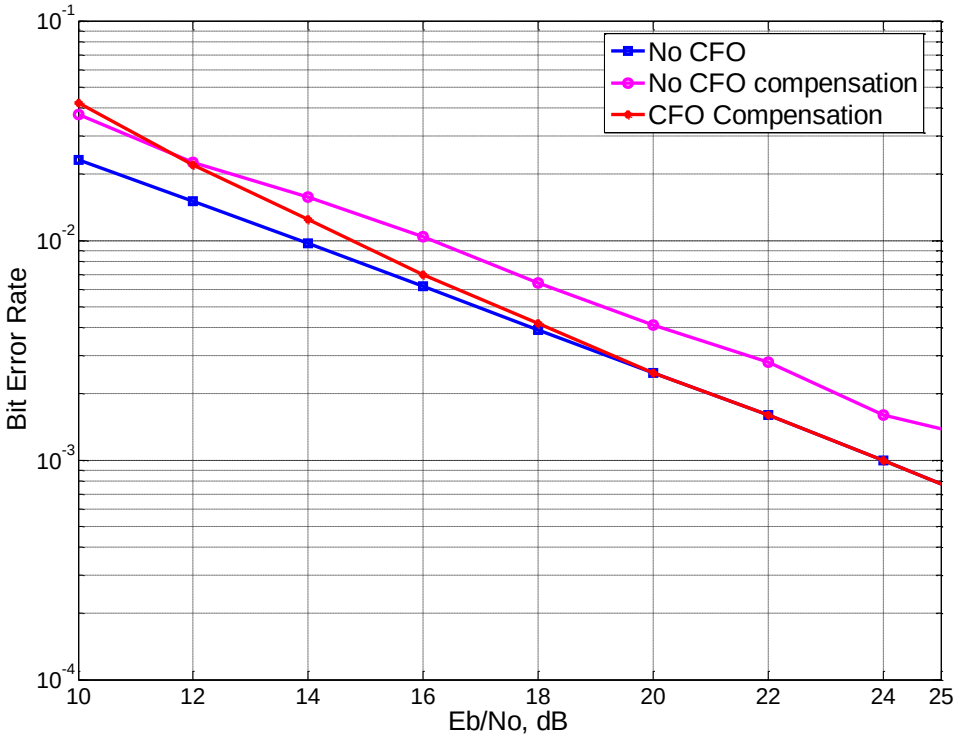

Figure 2.12: Comparison of BER among methods.

CHAPTER 3

CHANNEL ESTIMATION IN HSR BASED ON COMPRESSED SENSING

In this chapter, theoritical background, system model and simulation results of Channel estimation based on Compressed sensing are examined.

3.1. Compressed sensing

Various traditional approaches to sampling signals or images are based on Shannon's well-known theorem: the sampling rate must be at least twice the maximum frequency of the original signal (the so-called Nyquist rate). Apparently, Shannon-Nyquist sampling principle lies behind nearly all signal acquisition used in consumer audio and visual electronics, medical imaging devices, radio receivers, etc. In the area of data conversion, for instance, standard analog-to-digital converter (ADC) technology applies the usual quantized Shannon representation - the signal is uniformly sampled above or at the Nyquist rate.

The principle of compressed sensing, also called compressive sensing, is a new sensing/sampling example that goes against the common belief in the field of data acquisition. CS theory states that one can rebuild certain signals and images from far fewer samples or measurements than conventional methods use. To realize this, CS is based on two principles: sparsity, which is related to the signals of interest, and incoherence, which pertains to the sensing modality.

Sparsity holds the idea that the "information rate" of a continuous time signal may be much smaller than its bandwidth capacity. Or in case of discrete-time signal, sparsity means the signal's number of degrees of freedom is relatively much smaller than the signal's finite length. More exactly, CS exploits the knowledge that many natural signals are sparse or compressible in the sense that they have concise or compact representations when characterized by a certain proper basis ψ.

Incoherence is related to the duality between time and frequency and demonstrates the idea that objects having a sparse representation in ψ must be spread out in the domain in which they are recored. For instance, a Dirac or a spike in the time domain is spread out in the frequency domain. In othre words, incoherence declares that different from the signal of interest, the sampling/sensing waveforms have an extremely dense representation in ψ.

The essential observation is that one is able to design efficient sensing and sampling protocols that catch the meaningful information content, embed in a sparse representation and condense it into a small amount of data. These are nonadaptive protocols and we only need to correlate the signal with a small number of fixed waveforms or basis which are incoherent with the sparsifying basis. What is most significant about these sampling protocols is that they allow a sensor to very efficiently measure the data in a sparse signal without trying to understand that signal. Furthermore, there is a method to apply numerical optimization to recover the full-length signal from the smaller amount of collected data. To put differently, CS is a very simple and efficient signal acquisition technique which samples the data at a low rate and later performs computational power for reconstructing from what seems to be an incomplete set of measurements.

3.2. Mathematical background of Compressed sensing

Mathematically speaking, we have a vector $f \in R^N$ which we expand in an orthonormal basis $\psi = [\psi_1, \psi_2, \cdots, \psi_N]$ as follows:

$$f = \sum_{i=1}^{N} x_i \psi_i, \tag{3.1}$$

where x is the coefficient sequence of f: $x_i = \langle f, \psi_i \rangle$. It will be convenient to represent $f = \psi x$ (where ψ is the $N \times N$ matrix with $\psi_1, \psi_2, \cdots, \psi_N$ as columns). In our context, we condiser f to be a S-sparse signal in ψ, which means there are at most S number of x_i is different from zero.

Our concern is reconstructing f from K number of observations y_k (K<N) of in another orthonormal basis $\theta = [\theta_1, \theta_2, \cdots, \theta_N]$:

$$y_k = \langle f, \theta_k \rangle, \quad k = 1, \dots, K. \tag{3.2}$$

Ideally, we would like to measure all the N coefficients of f. However, in case $S << N$ and ψ is low coherent with θ as in [42], we can fully reconstruct f if certain value of K < N by L1-norm minimization. The proposed reconstruction f^* is given by $f^* = \psi x^*$, where $x^*$is the solution to the convex optimization program ($\|x\|_{L1} := \sum_i |x_i|$):

$$\min \|\tilde{x}\|_{L1} \ subject\ to\ y_k = \langle f, \psi \tilde{x} \rangle, \quad \forall k = 1, \dots, K. \tag{3.3}$$

That is, among all objects $\tilde{f} = \psi \tilde{x}$ consistent with the data, we select that whose coefficient sequence has minimal L1-norm.

Fig.3.1 illustrates an example of the above algorithm. The original signal is taken in time domain with N=256 points of data - $x \in R^{256}$. There are K=64 observations of x is conducted through the generated randomly measurement matrix A (64×256): $y = Ax$. As shown in the figgure, the original signal had 256 values but we recovered it perfectly even though we only took 64 random measurements.

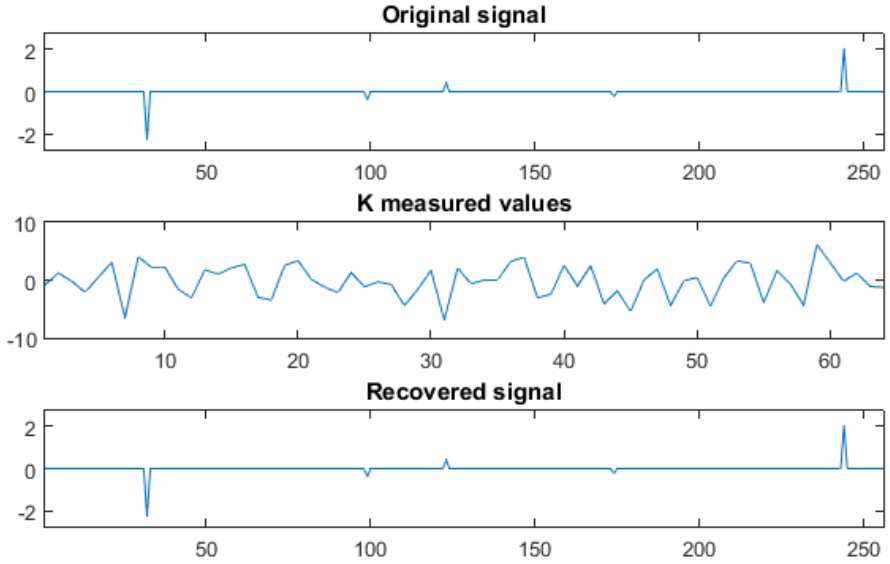

Figure 3.1: Example of recovering signal with compressed sensing.

3.3. Channel estimation based on compressed sensing

In this chapter, we consider an OFDM system similar to the system in chapter 2.3 (one RRU and one MS). The channel estimation here is based on pilot. As in chapter 2.1, we have one the received symbol is:

$$y = \boldsymbol{E}(\varphi)\boldsymbol{W}_P\boldsymbol{H_P}s. \tag{3.4}$$

Considering all data slot in s, we can modify (3.4) as:

$$y = \boldsymbol{E}(\varphi)\boldsymbol{W}\boldsymbol{H}s. \tag{3.5}$$

As denoted in 2.1, we have $\boldsymbol{h}$ is channel impulse response. Denote:

$$\boldsymbol{S} = diag[s(1) \dots s(N)] \text{ and } Y = \boldsymbol{W}y. \tag{3.6}$$

As shown in [43] We have (3.5) is equivalent to:

$$Y = \boldsymbol{S}\boldsymbol{W}\boldsymbol{E}(\varphi)\boldsymbol{h}. \tag{3.7}$$

Suppose that there are Pi pilot subcarriers, and Γ is the $Pi \times N$ selection matrix that selects the pilot locations of the symbol. We denote $\boldsymbol{S}_{Pi}$ and Y_{Pi} the known pilot data at the transmitter and the received data at the corresponding subcarriers. As a result, we have $\boldsymbol{S}_{Pi} = \Gamma\boldsymbol{S}\Gamma^T$ and $Y_{Pi} = \Gamma Y$. The equation (3.7) is equivalent to:

$$\Gamma Y = \Gamma\boldsymbol{S}\Gamma^T\Gamma\boldsymbol{W}\boldsymbol{E}(\varphi)\boldsymbol{h}$$

$$\leftrightarrow Y_{Pi} = \boldsymbol{S}_{Pi}\Gamma\boldsymbol{W}\boldsymbol{E}(\varphi)\boldsymbol{h} \tag{3.8}$$

$$\leftrightarrow Y_{Pi} = \boldsymbol{A}\boldsymbol{E}(\varphi)\boldsymbol{h}. \tag{3.9}$$

In HSR OFDM, with large N, we can consider $\boldsymbol{h}$ to be sparse since the number of dominated propagation paths is small relative to N. Although, matrix $\boldsymbol{E}(\varphi)$ shifts the frequencies of $\boldsymbol{h}$, it does not break its sparsity. Consequently, $\boldsymbol{E}(\varphi)\boldsymbol{h}$ can be considered as sparse.

Up to this point, at the receiver, we know the measured sample Y_{Pi}, the measurement matrix $\boldsymbol{A}$ and we also comprehend the sparsity of $\boldsymbol{E}(\varphi)\boldsymbol{h}$. With the algorithm of CS in 3.1, we can reconstruct $\boldsymbol{E}(\varphi)\boldsymbol{h}$ through L1-minimization.

3.4. Simulation of channel estimation based on CS

Fig.3.2 is an example of recover channel impulse response through compressed sensing. In the example, one OFDM symbol with length of 128 is sent though a Rayleigh channel under carrier frequency shift. The two figures above in Fig.3.2 are the real and the imaginary parts of the channel impulse response with the assumption that there are 8 propagation paths (N_{Tap}) in the channel. The two figures below are the recovered real and imaginary parts based in compressed sensing algorithm, exploiting the knowledge of 128/4=32 pilots subcarriers.

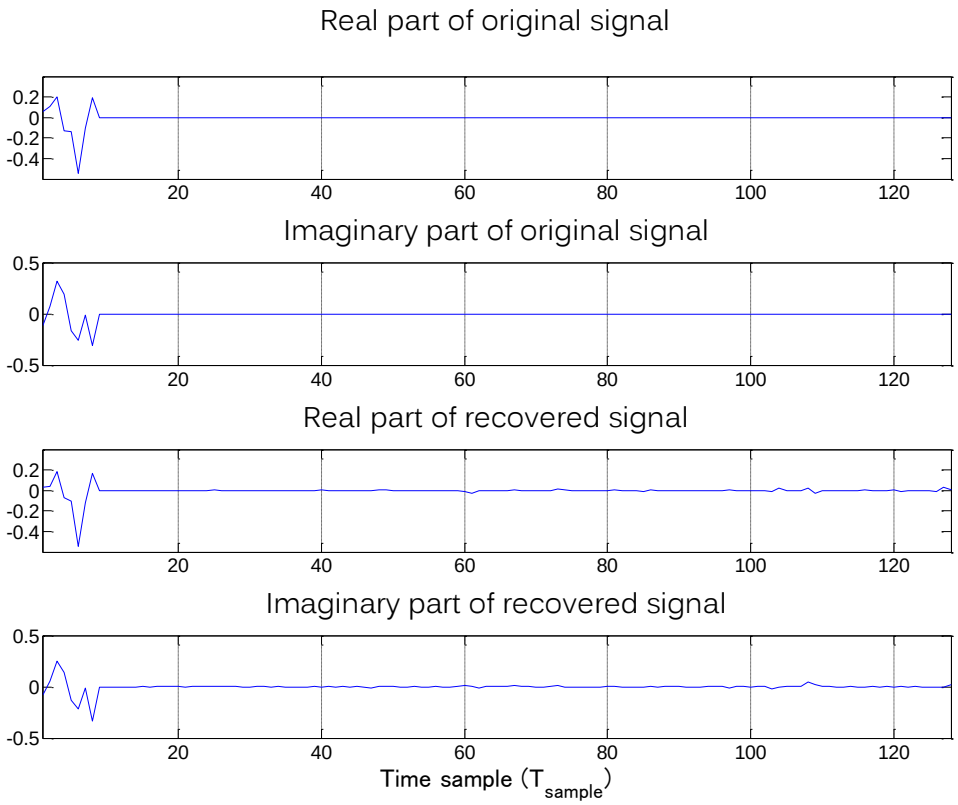

Figure 3.2: Recovering channel impulse response with compressed sensing in case of N=128,Eb/N0=25dB and $N_{Tap} = 8$.

Fig.3.3 is the Mean square error of the estimation. As expected from the theory of Compressed sensing, the more non-zero unknowns, the harder to recover the signal from a certain number of equations. As N_{Tap} increases (from 4 to 12), the MSE gets greater. However, this problem can be solved in HSR-OFDM of 2 following reasons:

1) Since the train usually travels in rural area, where scatterers are few and the distance between RRU and the train, d_B in Fig.1.4, is short, the signal energy mainly aggregates at the line of sight (LOS) path. In that situation, the channel can be considered having only one propagation path.
2) Typical values for delay spread in open area is less than 0.2 μs and it is less than 3μs in urban area, while the symbol duration in our scenario and the scenario in [for Minh] is 67 μs; which means the dominated taps are located among 6 first sample of the 128 points impulse response. Thus most of the time, N_{Tap} is less than 7.

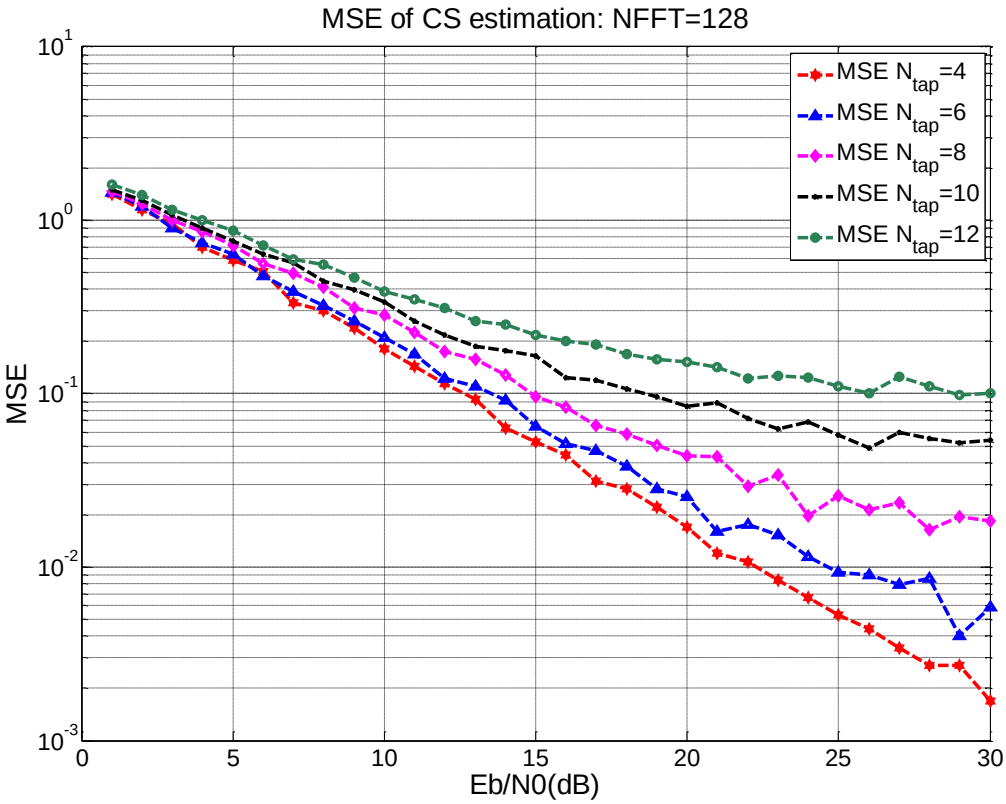

Figure 3.3: Mean square errors of CS Channel estimation.

3.5. Future works based on manifold approximation

Most of our works in section 3.2 and 3.3 are based on the assumption that all the taps of channel impulse response are either dominated tap or zero. In fact, that assumption is not true. The "zero" taps actually have certain power and they have impact on the system. Thus, if we can estimate them accurately, we can further enhance the system performance.

Our solution in section 3.2 and 3.3 can be considered as a lower resolution of the real channel impulse response. The problem, hence, is similar to the process of recovering high resolution image from low resolution version of it. One promising approach is the usage of subspace clustering and manifold approximation as shown in [44].

Subspace clustering considers the problem of modeling a collection of data points with a union of subspaces [17]. The main idea of SSC was developed from the self-expressive property where the set of N high dimensional vector points in R^D(normally N >> D), denoted by $H = \{h_j \in R^D\}_{j=1}^N$ used as a dictionary itself for sparse representation to create an affinity matrix. In particular, the set of vector points could be written in a matrix form $H = [h_1, h_2, \dots, h_N] \in R^{D \times N}$. Let $H_i = H/\{h_i\}$ be the matrix obtained from H by removing its i-th column. The self-expressive property implies looking for a sparse representation of hi from its corresponding dictionary H;. According to the theory of compressive sensing, a sparse solution could be found via L1 norm minimization. After finding the sparse representation of every column of the data matrix H, the data has been segmentation into subspaces.

Manifold approximation is the process of selecting an element derived from a certain set based on a representation of an object. The chosen element is based on the distance between the representation and the subspace containing the chosen element and other elements in the set. This method of approximation has shown its potential in [44].

Based on subspace clustering and manifold approximation, our project in the near future can be illustrated as following steps:

1) Constructing a library of channel impulse response corresponding to the communiation link beforehand (denoted $\boldsymbol{H_{lib}} = \{\ddot{\boldsymbol{H}}_{\boldsymbol{i}}\}, \forall \boldsymbol{i}$). Eace element of $\boldsymbol{H_{lib}}$ is extracted into two parts; the first $\boldsymbol{H_{lib-D}}$ containing all the the dominated taps (or, more precisely, the taps in the delay spread region) of all elements of $\boldsymbol{H_{lib}}$ ($\boldsymbol{H_{lib-D}} = \{\ddot{\boldsymbol{H}}_{\boldsymbol{i-D}}\}, \forall \boldsymbol{i}$) and $\boldsymbol{H_{lib-0}}$ containing the remaining taps of $\boldsymbol{H_{lib}}$ ($\boldsymbol{H_{lib-0}} = \{\ddot{\boldsymbol{H}}_{\boldsymbol{i-0}}\}, \forall \boldsymbol{i}$)
2) Applying subspace clustering algorithm to divide $\boldsymbol{H_{lib}}$ into subspaces.
3) Recovering low resolution $\boldsymbol{h_L}$ version of channel impulse response as in section 3.2 and 3.3 with the assumption that the non-dominated taps are zeros.
4) Extracting the dominated region of the recovering channel impulse response (denoted $\boldsymbol{h_{L-D}}$).
5) Applying manifold approximation to find the high resolution dominated region of channel impulse response $\boldsymbol{h_{H-D}}$ in $\boldsymbol{H_{lib-D}}$ from $\boldsymbol{h_{L-D}}$.
6) Finding the corresponding $\boldsymbol{h_{H-0}}$ corresponding to $\boldsymbol{h_{H-D}}$ in the library and recover $\boldsymbol{h_H}$.

CHAPTER 4

DEVELOPMENT OF OFDM SYSTEM USING CHAOTIC SUBCARRIERS

In this chapter, theoritical background, system model and simulation results of Chaotic subcarriers interleaving are examined.

4.1. Chaotic mapping and discretized Baker Map

A chaotic map is a map that possesses some sort of chaotic behavior. Map may be parameterized by a discrete-time or continuous-time parameter. Fig.4.1 shows a square image consisting of NxN pixels. It is divided vertically into k rectangle-shaped parts with size of p1, p2... pk respectively. The vector (p1, p2… pk) is call Baker key.

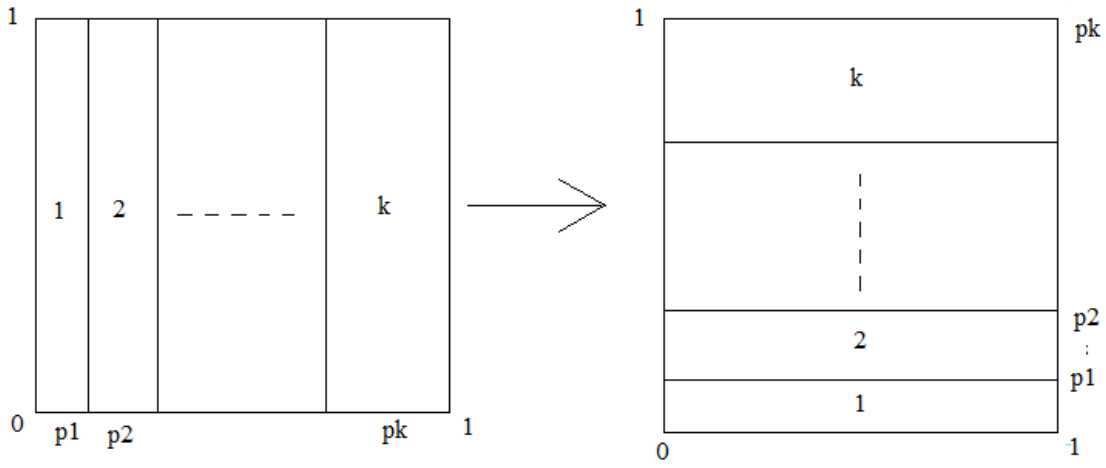

Figure 4.1: Generalize Baker map.

Discretized Baker Map (DBM) is commonly used in image encryption. In such applications, DBM is classified into two versions: A and B. In this project, version A is concerned. The formula of version A is:

$$B(x', y') = A\left(\frac{N}{p_i}(x - P_i) + y \bmod \frac{N}{p_i},\ \frac{p_i}{N}\left(y - y \bmod \frac{N}{p_i}\right) + P_i\right), \qquad (4.1)$$

where $P_i = p_1 + p_2 + \cdots + p_i$; $N = p_1 + p_2 + \cdots + p_k$; $P_i \le x < P_i + p_i$.

Fig.4.2 shows the case in which N = 8 with the Baker key equals to (2, 4, 2).

The chaotic interleaving is performed as follows [33]:

1) An NxN square matrix is divided into k vertical rectangles of height N and width p_i.
2) These vertical rectangles are stretched in the horizontal direction and contracted vertically to obtain a p_i x N horizontal rectangle.
3) These rectangles are stacked as shown in Fig.2, where the left one is put at the bottom and the right one at the top.
4) Each p_i × N vertical rectangle is divided into p_i boxes of dimensions $N=p_i \times p_i$ containing exactly N points.
5) Each of these boxes is mapped column by column into a row as shown in Fig.4.2.

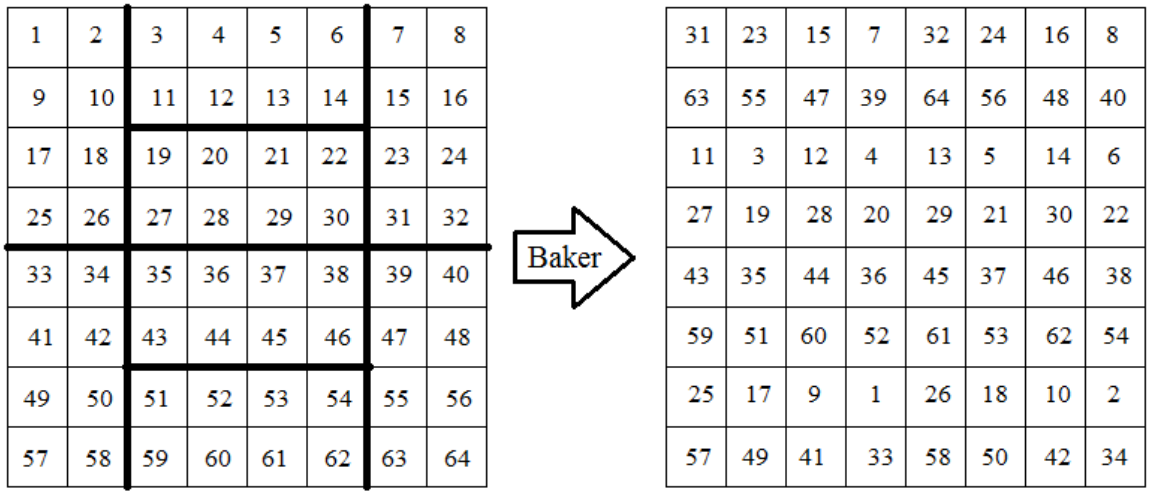

Figure 4.2: Version A of DBM – key = (2,4,2).

4.2. Proposed OFDM system with chaotic subcarriers

The proposed OFDM system add a block named IDFT with DBM at transmitter and a DFT with DBM at receiver as shown in Fig.4.3. This two blocks' difference with the conventional IDFT/DFT blocks is the implementation of the chaotic subcarriers modulation.

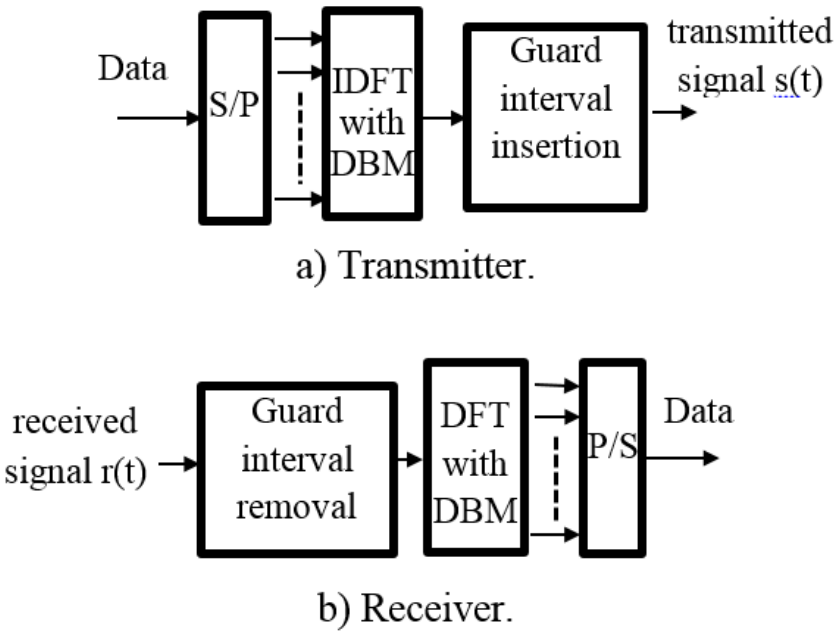

Figure 4.3: The proposed OFDM system.

In convenional OFDM, multiple sinusoidal with frequency separation 1/ T_s is used where T_s is the symbol duration. Denote c_k, f_k and s(t) the information symbol, the frequency of the subcarrier and the OFDM signal, respectively. The m^{th} ($m \in [1, N]$) sample of s(t) is:

$$s_m = \sum_{k=1}^{N} c_k . e^{j2\pi f_k \frac{(m-1)T_S}{N}}, \quad (4.2)$$

In this system, we use 8x8 matrix DBM as in Fig.4.1. The 1st element is mapped to the 31st, the 2nd to the 23rd …, and the 64th to the 34th . When N=64, equation (4.2) becomes:

$$s_m = c_1 . e^{j2\pi f_1 \frac{(m-1)T_S}{N}} + c_2 . e^{j2\pi f_2 \frac{(m-1)T_S}{N}} + \cdots + c_{64} . e^{j2\pi f_{64} \frac{(m-1)T_S}{N}}, \quad (4.3)$$

Applying DBM in subcarriers we have: f_1 maps to f_{31}, f_2 maps to f_{23}…, and f_{64} maps to f_{34} (mapping is shown in Fig.4.2). We get a new OFDM system and equation (4.3) becomes:

$$s_m = c_1 . e^{j2\pi f_{31}\frac{(m-1)T_S}{N}} + c_2 . e^{j2\pi f_{23}\frac{(m-1)T_S}{N}} + \cdots + c_{64} . e^{j2\pi f_{34}\frac{(m-1)T_S}{N}} . \qquad (4.4)$$

The transformation of transmitted signal from equation (4.3) to equation (4.4) is presented in Fig.4.4a and the reallocating subcarriers of received signal is showed in Fig.4.4b

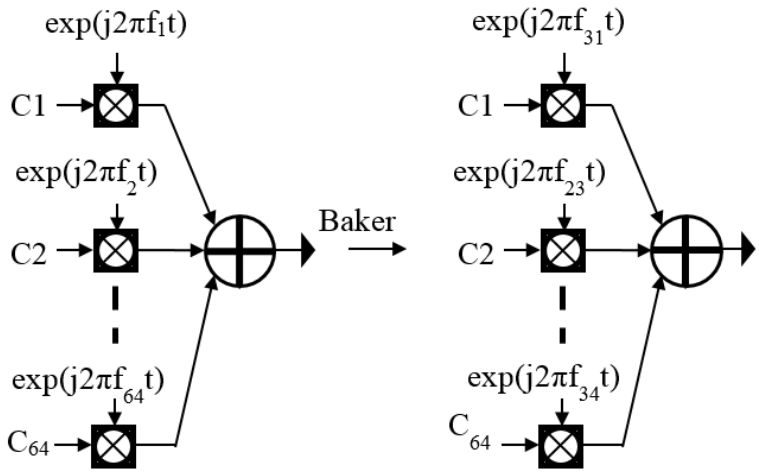

a) Subcarriers in transmitter of the conventional OFDM system and the prosed OFDM system.

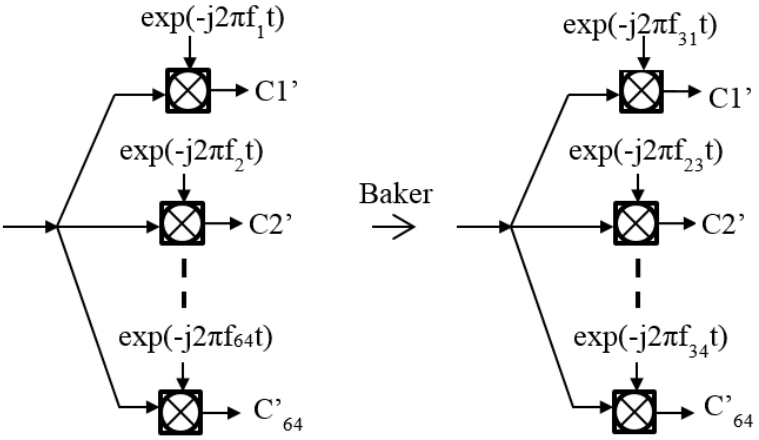

b) Subcarriers in receiver of the conventional OFDM system and the prosed OFDM system.

Figure 4.4: Mapping subcarriers.

"IDFT with DBM" block and "DFT with DBM" block which allocate subcarriers based on DBM are implemented as described in Fig.4.4. In case there are more than 64 subcarriers (128, 256…), the subcarriers are divided into smaller groups of 64 subcarriers and processed as above.

4.3. Simulation of chaotic subcarrier interleaving

In an OFDM transmission, the transmission of cyclic prefix does not carry 'extra' information. The signal energy is spread over time $T_d + T_{CP}$ whereas the bit energy is spread over the time T_d.

$$E_s.(T_d + T_{CP}) = E_b.T_d. \quad (4.5)$$

Simplifying (4.5) we have:

$$E_s = \frac{T_d}{T_d+T_{CP}} E_b. \quad (4.6)$$

In addition, not all the available subcarriers from the DFT are used for data transmission. Typically, some subcarriers are left unused to ensure spectrum roll off. Assume that we have N subcarriers and the number of used subcarriers is n. We have:

$$E_s = \frac{n}{N} E_b. \quad (4.7)$$

Combining the impacts of prefix (4.5) and unused subcarriers (4.6), the relation between symbol energy and the bit energy is:

$$\frac{E_s}{N_0} = \frac{E_b}{N_0}.\left(\frac{T_d}{T_d+T_{CP}}\right).\frac{n}{N}. \quad (4.8)$$

$$\frac{E_s}{N_0}[dB] = \frac{E_b}{N_0}[dB] + 10 * log\left(\frac{T_d}{T_d+T_{CP}}\right) + 10 * log\frac{n}{N}. \quad (4.9)$$

Consequently, we have:

$$\text{SNR[dB]} = E_s/N_0\,[dB] - 10 * log\frac{n}{N}. \quad (4.10)$$

Theoretical BER:

$$P_e = 2 * Q\left(\frac{E_S}{N_0}\right). \quad (4.11)$$

From (4.9) and (4.11), we can see that BER of OFDM using QPSK does not depend on the order of symbols or subcarriers.

In the simulations, signal is transmitted using conventional OFDM and proposed OFDM over an additive white Gaussian noise (AWGN) channel. QPSK is used for baseband modulation. There are 64 subcarriers and guard interval length equals to a quarter of the symbol duration. The result of this simulation is shown in Fig.6. It shows that there is little difference in BER between the conventional OFDM system and the proposed OFDM system caused by AWGN.

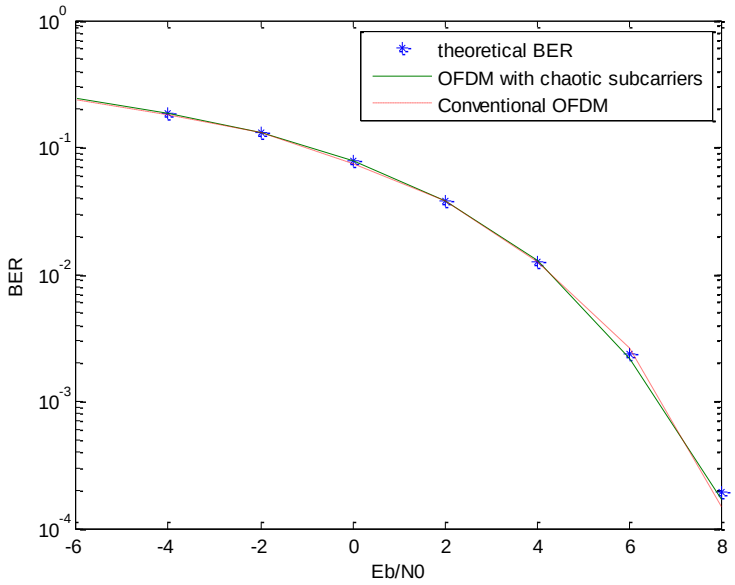

Figure 4.5: Theoretical BER, BER of conventional OFDM and OFDM with chaotic subcarriers under AWGN channel.

As shown in Fig.4.5, BER of the conventional OFDM and the proposed OFDM are not much different. This means mapping subcarriers do not deplete signal's quality. However, the proposed chaotic interleaving approach, apparently, adds a degree of encryption to the system.

In addition to AWGN channel, we also investigate our proposed method under the effect of Rayleigh fading. Fig.4.6 shows the comparison among BER of

theoretical analysis, OFDM chaotic and conventional OFDM. The simulation uses QPSK modulation with 64 subcarriers. The result showed small differences among scenarios, indicating chaotic-subcarriers does not reduce the precision of transmitting signals.

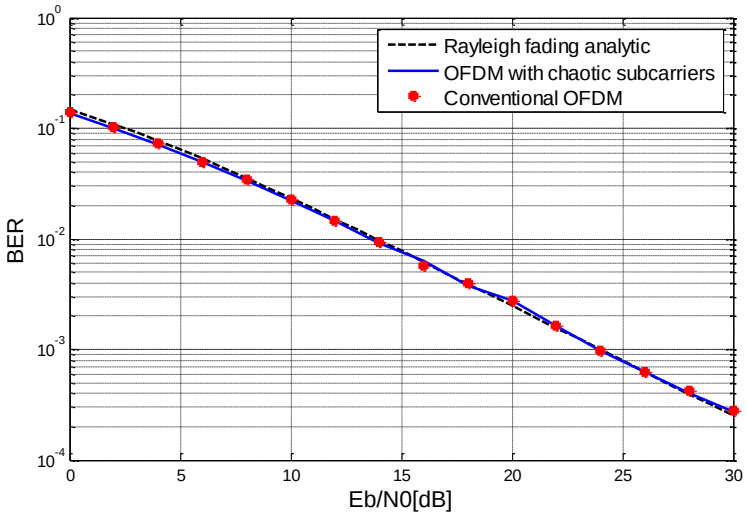

Figure 4.6: Theoretical BER, BER of conventional OFDM and OFDM with chaotic subcarriers under Rayleigh channel.

In Fig.4.7, we analyzed the influences of number of subcarriers on BER under Rayleigh fading channel. Due to the fact that an equalizer is applied at receiver and Doppler Effect is neglected, there are minor differences among schemes.

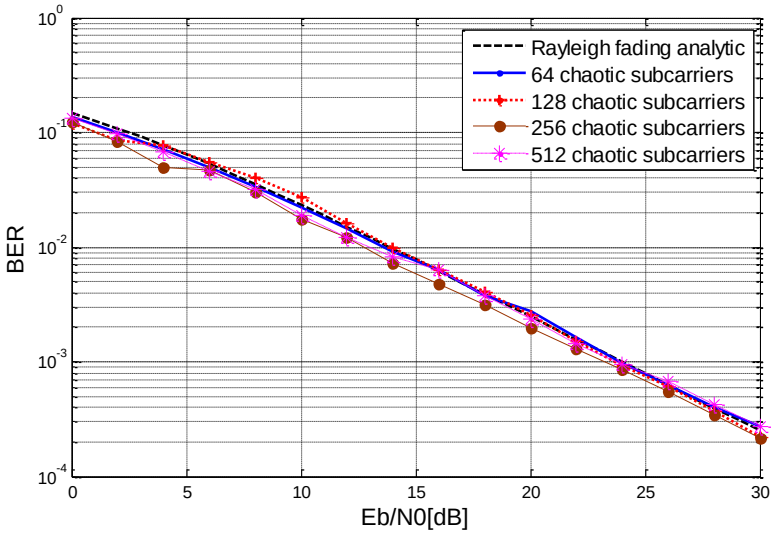

Figure 4.7: Theoretical BER and BER of OFDM chaotic with different number of subcarriers under Rayleigh channel.

Lastly, we examine the proposed method under different modulation scheme. The results of 4-QAM, 16-QAM and 64-QAM in Rayleigh fading are compared with theoretical values in Fig.4.8. As illustrated in the figure, the BER of OFDM chaotic schemes are consistent with theoretical analysis which suggests that, even with varying modulation methods, chaotic mapping still maintains the reliability while improves the security of the signal.

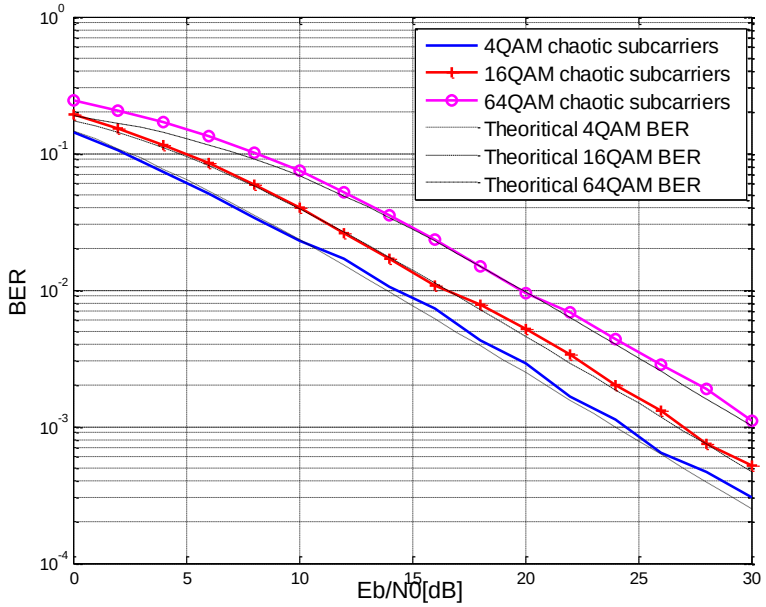

Figure 4.8: Theoretical BER and BER of OFDM chaotic with different modulation schemes under Rayleigh channel.

CONCLUSIONS AND PERSPECTIVES

To this point, we have investigated the issue of Doppler frequency shift in HSR-OFDM systems and examined a MUSIC based ICI mitigation scheme for two RRUs. We also proposed a research direction harvesting the application of compressed sensing and manifold approximation in OFDM channel estimation. In addition, a scheme of interleaving chaotic subcarriers modulation on OFDM symbol before transmission is introduced and examined.

For future works, we are planning to realize our propose in compressed sensing based channel estimation as in 3.5.

REFERENCES

[1] Y. Zhou, Z. Pan, J. Hu, J. Shi, and X. Mo, "Broadband wireless communications on high speed trains," in Annual Wireless and Optical Communications Conference (WOCC), Apr. 2011, pp.1-6.

[2] C. Yang, L. Lu, C. Di and X. Fang, "An On-Vehicle Dual-Antenna Handover Scheme for High-Speed Railway Distributed Antenna System," in Int. Conf. Wireless Communications Networking and Mobile Computing (WiCOM) , Sept. 2010, pp.1-5.

[3] H. Liu and U. Tureli, "A high efficiency estimator for OFDM communications," IEEE Commun. Lett., vol. 2, pp. 104-106, Apr. 1998.

[4] Stuber G L, Barry J R, McLaughlin S W, Li Y, Ingram M A, Pratt T G. Broadband MIMO-OFDM wireless communications. Proc.IEEE, 2004, 92(2): 271-294.

[5] Pollet T, Van Bladel M, Moeneclaey M. BER sensitivity of OFDM systems to carrier frequency offset and Wiener phase noise. IEEE Trans. Commun., 1995, 43(234): 191-193.

[6] Moose P H. A technique for orthogonal frequency division multiplexing frequency offset correction. IEEE Trans. Commun., 1994, 42(10): 2908-2914.

[7] Yu J H, Su Y T. Pilot-assisted maximum-likelihood frequency-offset estimation for OFDM systems. IEEE Trans. Commun., 2004, 52(11): 1997-2008.

[8] Roman T, Koivunen V. Subspace method for blind CFO estimation for OFDM systems with constant modulus constellations. In: Proc. IEEE VTC. Stockholm, Sweden, 2005: 1253-1257.

[9] Yang F, Li K H, Teh K C. A carrier frequency offset estimation with minimum output variance for OFDM systems. IEEE Commun.Lett., 2004, 8(11): 677-679.

[10] Van Zelst A, Schenk T C W. Implementation of a MIMO OFDM based wireless LAN system. IEEE Trans.Signal Process. 2004, 52(2): 483-494.

[11] Jiang Y, Gao X, You X, Heng W. Training sequence assisted frequency offset estimation for MIMO OFDM. In: Proc. IEEE ICC. Istanbul, Turkey, 2006: 5371-5376.

[12] Van de Beek J J, Sandell M, Brjesson P O. ML estimation of timing and frequency offset in OFDM systems. IEEE Trans. Signal Process. 1997, 45(7): 1800-1805.

[13] R4-060383, "Further considerations on high speed train environment," Siemens, 3GPP RAN4 # 39.

[14] Y. Jiang, G. Zhu and Z. Wang, "A specific mobile relay with Doppler diversity in OFDM system for high-speed railway scenario", in 2nd IEEE Int. Conf. on Network Infrastructure and Digital Content, Sept.2010, pp. 742-747.

[15] Ralph O, Schmidt. Multiple Emitter Location and signal Parameter Estimation. IEEE Trans. On Antennas and Propagation, March 1986. Vol. 34. No. 3. pp 276-280.

[16] E. J. Candès, J. Romberg, and T. Tao. Stable signal recovery from incomplete and inaccurate measurements. Communications on Pure and Applied Mathematics, 59(8):1207-1223, 2006.

[17] R. Vidal, "Subspace clustering", IEEE Signal Process. Mag., vol. 28, no. 2, pp. 52-68, 2011.

[18] P. Sun and L.Zhang, "Low complexity pilot aided frequency synchronization for OFDMA uplink transmissions," IEEE Trans. Wireless Commun., vol. 8, no. 7, pp. 3758–3769, Jul. 2009.

[19] L. Bai and Q. Yin, "Frequency synchronization for the OFDMA uplink based on the tile structure of IEEE 802.16e," IEEE Trans. Veh. Technol., vol. 61, no. 5, pp. 2348–2353, Jun. 2012.

[20] O. Besson and P. Stoica, "On parameter estimation of MIMO flat-fading channels with frequency offsets," IEEE Trans. Signal Process. vol. 51, no. 3, pp. 602–613, 2003.

[21] Y. Zeng, R. A. Leyman, and T. S. Ng, "Joint semiblind frequency offset and channel estiamtion for multiuser MIMO-OFDM uplink," IEEE Trans. Commun., vol. 55, no. 12, pp. 2270–2278, 2007.

[22] J. Chen, Y. C. Su, S. Ma, and T. S. Ng, "Joint CFO and channel estimation for multiuser MIMO-OFDM systems with optimal training sequences," IEEE Trans. Signal Process., vol. 56, no. 8, pp. 4008–4019, 2008.

[23] Y. Wu, J. W. M. Bergmans, and S. Attallah, "Carrier frequency offset estimation for multiuser MIMO OFDM uplink using CAZAC sequences: performance and sequence optimization," EURASIP Journal on Wirel. Commun. and Network., vol. 2011, Article ID: 570680.

[24] Y. Jiang, X. Zhu, E. Lim, Y. Huang, and H. Lin, "Low-complexity semiblind multi-CFO estimation and ICA-baed equalization for CoMP OFDM systems," IEEE Trans. Vehicular Technology, vol. 63, no. 4, pp. 1928–1934, May 2014.

[25] J. Xiong , L. Gui , H. Liu and P. Cheng, "On channel estimation and equalization in 2x1 MISO TDS-OFDM based terrestrial DTVsystems", IEEE Trans. Broadcast., vol. 58, pp. 130-138, 2012.

[26] R.G. Baranluk, Compressive sensing. IEEE Signal Process. Mag.24 (4), 118–121 (2007).

[27] E.J. Candès, J. Romberg, T. Tao, Robust uncertainty principle: Exact signal reconstruction from highly incomplete frequency information. IEEE Trans. Inf. Theory52 (2), 489–509 (2006).

[28] D.L. Donoho, Compressed sensing. IEEE Trans. Inf. Theory52 (4), 1289–1306 (2006).

[29] W. Bajwa, J. Haupt, A. Sayeed, R. Nowak, Compressed channel sensing: a new approach to estimating sparse multipath channels. Proc. IEEE98 (6), 1058–1076 (2010).

[30] C.R. Berger, S. Zhou, J.C. Preisig, P. Willett, Sparse channel estimation for multicarrier underwater acoustic communication: from subspace methods to compressed sensing. IEEE Trans. Signal Process. 58(3), 1708–1721 (2010).

[31] G. Taubock, F. Hlawatsch, D. Eiwen, H. Raunhut, Compressive estimation of doubly selective channels in multicarrier systems: leakage effects and sparsity-enhancing processing. IEEE J. Sel. Top. Signal Process.4 (2), 255–271 (2010).

[32] Y.Mao, G.Chen, S.Lian, "A novel fast image encryption scheme based on 3D chaotic Baker maps", Int. J. Bifurcation Chaos, Vol. 14, No. 10 (2004) 3613-3624.

[33] E.M.El-Bakary, O.Zahran, S.A.El-Dolil, F.E.Abd El-Samie, "Chaotic Maps: A tool to enhance the performance of OFDM Systems", International Journal of Communication Networks and Information Security**,** Vol. 1, No. 2, August 2009.

[34] F.Huang, Y.Feng, "Security analysis of image encryption based on two-dimensional chaotic maps and improved algorithm", Frontiers of Electrical and Electronic Engineering in China, Volume 4, Issue 1, p.5-9.

[35] D.Luengo, Ignacio Santamaría, "Secure Communications Using OFDM with Chaotic Modulation in the Subcarriers", Vehicular Technology Conference, 2005. VTC 2005-Spring. 2005 IEEE 61st, p.1022-1026 Vol.2.

[36] M. P. Kennedy, R. Rovatti, and G. Setti, Eds., Chaotic Electronics in Telecommunications. CRC Press, 2000.

[37] F.C.M.Lau and C.K.Tse, Chaos-Based Digital Communication Systems. Berlin: Springer-Verlag, 2003.

[38] S.K.Kadari, B.S.B.Raju, N.X.Quyen, "Digital image encryption based on chaotic behavior of a modified tent map", ISAST transactions on computer and intelligent system, No.1, Vol.4, 2012 (ISSN 1798-2448).

[39] N.F. Soliman, A.A. Shaalan, S. El-Rabaie, and F.E. Abd El-samie, "Peak power reduction of OFDM signals using chaotic Baker map", In proceedings IEEE International Conference on Computer Engineering & Systems, 2009. ICCES 2009, p.593-598.

[40] H. Sari, G. Karam, and I. Jeanclaude, "Transmission techniques for digital terrestial TV broadcasting,"IEEE Commun. Mag., vol. 33, no. 2, pp. 100–109, Feb. 1995.

[41] 3GPP TR 36.211 v8.6.0., "Physical Channel and Modulation for Evolved UTRA[S]".2009.

[42] E. J. Candès, and M. B. Wakin, "An Introduction To Compressive Sampling," IEEE Signal Proc Mag., 25: 21-30, 2008.

[43] X. P. Zhou, Y. Fang, M. Wang, "Compressed sensing based Channel estimation for Fast Fading OFDM systems, " Journal of System Engineering and Electronics, Vol. 21, No. 4, pp. 550-556, August 2010.

[44] C. Dang , M. Aghagolzadeh , A. Moghadam and H. Radha, "Single image super-resolution via manifoldlinear approximation using sparse subspace clustering", Proc.IEEE Global Conf. Signal and Information Processing, pp. 949-953, 2013.